(2)

ADAPTIVE CONTROL OF HELICOPTER VIBRATIONS VIA THE IMPULSE RESPONSE METHOD

A Final Report

Submitted by:

Carl R. Knospe
Graduate Student

J. K. Haviland
Professor

W. D. Pilkey
Frederick Tracy Morse Professor

June 1, 1986 - May 31, 1989

Submitted to:

U. S. Army Research Office
P. O. Box 12211
4300 S. Miami Boulevard
Research Triangle Park, NC 27709

ARO No. DAAL03-86-G-0043

Report No. UVA/525167/MAE90/101
September 1989

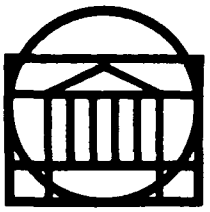

SCHOOL OF ENGINEERING AND APPLIED SCIENCE
DEPARTMENT OF MECHANICAL AND AEROSPACE ENGINEERING

UNIVERSITY OF VIRGINIA
CHARLOTTESVILLE, VIRGINIA 22901

UNIVERSITY OF VIRGINIA
School of Engineering and Applied Science

The University of Virginia's School of Engineering and Applied Science has an undergraduate enrollment of approximately 1,500 students with a graduate enrollment of approximately 600. There are 160 faculty members, a majority of whom conduct research in addition to teaching.

Research is a vital part of the educational program and interests parallel academic specialties. These range from the classical engineering disciplines of Chemical, Civil, Electrical, and Mechanical and Aerospace to newer, more specialized fields of Applied Mechanics, Biomedical Engineering, Systems Engineering, Materials Science, Nuclear Engineering and Engineering Physics, Applied Mathematics and Computer Science. Within these disciplines there are well equipped laboratories for conducting highly specialized research. All departments offer the doctorate; Biomedical and Materials Science grant only graduate degrees. In addition, courses in the humanities are offered within the School.

The University of Virginia (which includes approximately 2,000 faculty and a total of full-time student enrollment of about 17,000), also offers professional degrees under the schools of Architecture, Law, Medicine, Nursing, Commerce, Business Administration, and Education. In addition, the College of Arts and Sciences houses departments of Mathematics, Physics, Chemistry and others relevant to the engineering research program. The School of Engineering and Applied Science is an integral part of this University community which provides opportunities for interdisciplinary work in pursuit of the basic goals of education, research, and public service.

ADAPTIVE CONTROL OF HELICOPTER VIBRATIONS VIA THE IMPULSE RESPONSE METHOD

A Final Report

Submitted by:

Carl R. Knospe
Graduate Student

J. K. Haviland
Professor

W. D. Pilkey
Frederick Tracy Morse Professor

June 1, 1986 - May 31, 1989

Submitted to:

U. S. Army Research Office
P. O. Box 12211
4300 S. Miami Boulevard
Research Triangle Park, NC 27709

ARO No. DAAL03-86-G-0043

Department of Mechanical and Aerospace Engineering
SCHOOL OF ENGINEERING AND APPLIED SCIENCE
UNIVERSITY OF VIRGINIA
CHARLOTTESVILLE, VIRGINIA

Approved for Public Release; Distribution Unlimited

Report No. UVA/525167/MAE90/101
September 1989

Copy No. 12

REPORT DOCUMENTATION PAGE

1a. REPORT SECURITY CLASSIFICATION Unclassified	1b. RESTRICTIVE MARKINGS
2a. SECURITY CLASSIFICATION AUTHORITY	3. DISTRIBUTION/AVAILABILITY OF REPORT Approved for public release; distribution unlimited.
2b. DECLASSIFICATION/DOWNGRADING SCHEDULE	
4. PERFORMING ORGANIZATION REPORT NUMBER(S) UVA/525167/MAE90/101	5. MONITORING ORGANIZATION REPORT NUMBER(S) ARO 23761.2-EG-F
6a. NAME OF PERFORMING ORGANIZATION University of Virginia, Dept. of Mechanical and Aerospace Eng. 6b. OFFICE SYMBOL (If applicable)	7a. NAME OF MONITORING ORGANIZATION U. S. Army Research Office
6c. ADDRESS (City, State, and ZIP Code) Thornton Hall Charlottesville, VA 22903-2442	7b. ADDRESS (City, State, and ZIP Code) P. O. Box 12211 Research Triangle Park, NC 27709-2211
8a. NAME OF FUNDING/SPONSORING ORGANIZATION U. S. Army Research Office 8b. OFFICE SYMBOL (If applicable)	9. PROCUREMENT INSTRUMENT IDENTIFICATION NUMBER DAAL03-86-G-0043
8c. ADDRESS (City, State, and ZIP Code) P. O. Box 12211 Research Triangle Park, NC 27709-2211	10. SOURCE OF FUNDING NUMBERS PROGRAM ELEMENT NO. / PROJECT NO. / TASK NO. / WORK UNIT ACCESSION NO.
11. TITLE (Include Security Classification) Adaptive Control of Helicopter Vibrations Via the Impulse Response Method	
12. PERSONAL AUTHOR(S) Carl R. Knospe, J. K. Haviland, W. D. Pilkey	
13a. TYPE OF REPORT Final	13b. TIME COVERED FROM 6-1-86 TO 5-31-89
14. DATE OF REPORT (Year, Month, Day) 89- 6- 1	15. PAGE COUNT 71
16. SUPPLEMENTARY NOTATION The view, opinions and/or findings contained in this report are those of the author(s) and should not be construed as an official Department of the Army position, policy, or decision, unless so designated by other documentation.	
17. COSATI CODES FIELD / GROUP / SUB-GROUP	18. SUBJECT TERMS (Continue on reverse if necessary and identify by block number) Adaptive Control, Helicopter Vibration, Circulant Matrices, Periodic Dynamics

19. An adaptive blade control algorithm for helicopter vibration reduction is developed as an application of an impulse response control method. The method is based on an impulse response formulation which is applicable to any linear system with periodic dynamics. For such systems, a matrix of discretized impulse responses defines the relationship between sequences of inputs and outputs sampled throughout a period. Under a nearly constant control vector assumption, the impulse response matrix is shown to be full, and for constant dynamics plants,

20. DISTRIBUTION/AVAILABILITY OF ABSTRACT ☒ UNCLASSIFIED/UNLIMITED ☐ SAME AS RPT. ☐ DTIC USERS	21. ABSTRACT SECURITY CLASSIFICATION Unclassified
22a. NAME OF RESPONSIBLE INDIVIDUAL	22b. TELEPHONE (Include Area Code) / 22c. OFFICE SYMBOL

belong to a class of matrices diagonalizable by Fast Fourier transforms, the circulant matrices. For systems with periodic input coefficients, a circulant/diagonal structure results. Such structures are shown to act as a theoretical link between impulse response control methods and frequency domain techniques.

In the investigation of adaptive helicopter vibration control presented, a vertical–axis–only plant is simulated by a model composed of an impulse response matrix and an uncontrolled vibration vector. The adaptive control is implemented by a regulator composed of an estimator and a controller. The model parameters are identified by either Kalman or batch weighted least squares (WLS) filtering in either global or local form. The resulting estimates are used in an optimal control law obtained by the minimization of a constrained, single–step, quadratic performance function. Four control laws are derived: global certainty–equivalent, local certainty equivalent, global cautious, and local cautious.

The filters derived are examined in open loop simulations to determine their identification capabilities independent of the control feedback. Two levels of open loop control variation are used to evaluate estimation performance with constant and time–varying plants. The Kalman filters are found to produce lower estimate errors than the WLS filters.

Closed loop simulations of the regulators are then conducted with the filters retuned. The global Kalman filter certainty–equivalent regulator produced the best overall vibration reduction, typically better than 90%. In some tests, invariable regulators yielded promising results. Cautious regulators are found to be of no benefit. Control quadratic weight proved to hinder regulator performance while a small control–rate quadratic weight enhanced the vibration reduction for certain regulators. Control rank, measurement noise, and estimation enhancement are also examined in closed loop simulations.

When the Kalman filter regulator is used, the control constraint results in an unstable covariance eigenvalue. This behavior is shown to be due to insufficient control rank, a condition equivalent to a lack of persistency of excitation. The instability is illustrated both theoretically and experimentally. Two methods of preventing covariance instability, random probing insertion and covariance trace bounding, are discussed and demonstrated.

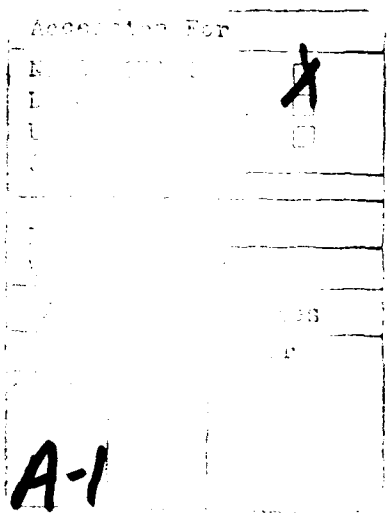

ACKNOWLEDGEMENTS

This research was funded by Army Research Office Contract No. DAAL03–86–G0043.

Notation

Vectors and Matrices

$\mathbf{A}(\cdot)$	Matrix in definition of linear first order system (Section 1.2)
$\mathbf{B}$	Diagonal matrix factor of impulse response matrix
$\mathbf{B}(\cdot)$	Matrix in definition of linear first order system (Section 1.2)
$\mathbf{C}$	Proposed circulant matrix factor of impulse response matrix
$\mathbf{C}(\cdot)$	Matrix in definition of linear first order system (Section 1.2)
$\mathbf{D}(\cdot)$	Matrix in definition of linear first order system (Section 1.2)
$\mathbf{F}$	Fast Fourier Transform matrix
$\mathbf{f}$	Vector forcing function (Section 1.2)
$\mathbf{G}$	Internal control rate weight matrix
$\mathbf{H}$	State propagation matrix
$\mathbf{H}_c$	Circulant Hermetian matrix
$\mathbf{I}$	Identity matrix
$\mathbf{K}$	Kalman gain vector
$\mathbf{L}$	Orthogonal transform (Section 1.8)
$\mathbf{M}$	Matrix relating measurement collection to parameter estimates
$\mathbf{P}$	Estimate error covariance matrix
$\mathbf{Q}$	Process noise covariance matrix
$\mathbf{R}$	Elementary impulse response matrix (unwrapped)
$\mathbf{T}$	Impulse response matrix
$\mathbf{U}_B$	Control batch matrix
$\mathbf{U}_f$	Infinite control collection matrix

Notation (Continued)

Vectors and Matrices (Cont'd)

$\mathbf{u}$	Control vector
$\underline{\mathbf{u}}$	Modified control vector
$\mathbf{v}$	Measurement noise vector
$\mathbf{W}$	Process noise covariance matrix
$\mathbf{W}_B$	Diagonal weight matrix (for batch WLS filter)
$\mathbf{w}$	Matrix of Gaussian zero mean numbers
$\mathbf{X}$	Vector in optimal control law
$\mathbf{x}$	Vector of vibrations
$\mathbf{x}_0$	Vector of uncontrolled vibration
$\mathbf{Y}$	State variable matrix
$\mathbf{Y}_B$	Measurement batch matrix
$\mathbf{y}$	Vector of vibration measurements
$\mathbf{Z}$	Matrix in optimal control law
$\mathbf{z}$	State vector (Section 1.2)
Φ	State transition matrix
Ψ	Orthogonal modes matrix
$\boldsymbol{\theta}$	Plant matrix
Π	Permutation matrix
ζ	*A priori* estimate error matrix
η	*A posteriori* estimate error matrix
Λ	Diagonal matrix of complex eigenvalues (Section 1.4) or Matrix of Lagrangian multipliers (Chapter 2)
ϵ	Error matrix in state propagation equation

Notation (Continued)

Scalars

b	Elements of diagonal matrix **B**
c	Elements of circulant matrix **C**
h	Elements of Hermetian circulant matrix $\mathbf{H}_c$
J	Performance function
m	Size of control vector
n	Size of measurement vector
r_1	Control weighting
r_2	Control–rate weighting
$u(\cdot)$	Control
V	Measurement noise covariance
$v(\cdot)$	Measurement noise
$w(\cdot,\cdot)$	Discretized impulse response element
$x(\cdot)$	Vibration
$x_o(\cdot)$	Uncontrolled vibration
$y(\cdot)$	Measurement
σ	Standard deviation
Ω	Blade rotational frequency
ϕ	Batch weight
λ	Eigenvalue
α	Batch weighting parameter
τ	Dummy time variable in convolution
ω	Elements of diagonal process noise matrix

Notation (Continued)

Superscripts

T	Matrix transform
-1	Matrix inverse
$\div$	Vector element inverse
$\bar{}$	*A priori* estimate
$\hat{}$	*A posteriori* estimate
$\sim$	Fast Fourier transform (Sections 1.4)

Subscripts

T	Referring to the impulse response matrix **T**
u	Referring to the control vector **u**
x	Referring to the uncontrolled vibration vector $\mathbf{x}_0$
θ	Referring to the plant matrix $\boldsymbol{\theta}$
v	Referring to the measurement noise **v**

TABLE OF CONTENTS

INTRODUCTION

The periodic aerodynamic loading of helicopter rotors leads to undesirable vibration levels throughout the aircraft. These vibrations result in pilot fatigue, passenger discomfort and greater maintenance and operating costs. For military helicopters, vibration also causes difficulty in aiming sights and pointing weapons. A reduction in operating vibration levels would therefore be of benefit to the military and commercial helicopter community.

The helicopter vibration problem can be attacked by two alternate strategies. In the first, the helicopter or components of it are isolated from the rotor so as to reduce the forces or the vibrations transmitted. The aerodynamic loading remains unchanged by such response attenuation devices. The second strategy, source alleviation, attempts to remove the periodic airloading through an azimuthal alteration of the blades' lifts. Response attenuation devices have been investigated extensively but are largely unsatisfactory due to their weight and insufficient robustness. Source alleviation methods have been employed and examined in a greater number of studies and have, in general, yielded promising results. Many of these approaches have included on–line system identification so that optimal vibration reduction can be achieved as the helicopter plant changes with flight condition [1–58]. In this report, an adaptive source alleviation controller is formulated in terms of a new input–output model. For any detail on this research effort, please see Reference 63.

CHAPTER ONE: THE IMPULSE RESPONSE METHOD AND ESTIMATION

1.1 Introduction

The impulse response method seeks to find a time sequence of discrete control inputs to the blades that will result in highly reduced fuselage vibrations. The method relies upon the quasi–periodic nature of the uncontrolled fuselage vibrations and the plant dynamics. This yields a predictable plant where previous measurements can be used to identify the periodic time sequences describing the uncontrolled vibration and the impulse response. The impulse response characterizes the plant dynamics. If the plant is linear (which it should be for small control amplitudes) then the control induced output is just the convolution of the impulse response and the control. Discretized, this, as shall be shown, takes the form of matrix relationship relating the control time sequence and the vibration time sequence. (If the flight condition is changing slowly, the plant is periodic, and the matrix has repeating blocks whose length is one period of the plant along its diagonal.) The matrix is identified by an estimator along with the uncontrolled vibration in some formulations. The estimates are then used by an optimal control law to compute a control sequence for the next plant period. For this research, the vibration reduction was to be obtained only on the vertical axis. This allows the same control sequence to be fed to each blade. (For multi–axis vibration reduction the blades must execute different control sequences simultaneously – see Reference 63.) Thus, at any time, all blades are executing the same deflection. The period of the plant in this case is one quarter revolution which in this study is called one cycle. Therefore, all control input sequences are harmonics of 4Ω. The controls commanded by this system could be carried out through a swashplate although this actuator would require a higher actuator bandwidth than on present helicopters.

For the multi–axis case, however, individual blade control must be used. In either case, the mechanics of blade control are not essential to the derivation of the vibration control system and are not considered here.

1.2 Impulse Response Method

For any linear system,

$$\dot{z}(t) = A(t)z(t) + B(t)f(t)$$

$$y(t) = C(t)z(t) + D(t)f(t) + v(t)$$

the response y(t) to a given forcing function is

$$y(t) = C(t)\left[\Phi(t,t_0)z(t_0) + \int_{t_0}^{t} \Phi(t,\tau)B(\tau)f(\tau)d\tau\right] + D(t)f(t) + v(t)$$

and for a system where the initial conditions have been damped out and the forcing term is the combination of a disturbance d(t) and a second derivative control u(t) the response takes the form

$$y(t) = D(t)d(t) \int_{t_0}^{t} C(t)\Phi(t,\tau)B(\tau)d(\tau)d\tau + D_2(t)u(t)$$
$$+ \int_{t_0}^{t} C(t)\Phi(t,\tau)B_2(\tau)u(\tau)d\tau + v(t)$$

If the disturbances $\mathbf{d}(t)$ and the impulse response $\mathbf{\Phi}(t,\tau)\mathbf{B}(t)$ were predictable, then an open loop control could be found to minimize a performance index of y and u. The response can be discretized by replacing the integrals with summations

$$y(t_j) = \mathbf{D}(t_j)\mathbf{d}(t_j) + \sum_{k=0}^{j} \mathbf{C}(t_j)\mathbf{\Phi}(t_j,t_k)\mathbf{B}(t_k)\mathbf{d}(t_k) + \mathbf{D}_2(t_j)u(t_j)$$
$$+ \sum_{k=0}^{j} \mathbf{C}(t_j)\mathbf{\Phi}(t_j,t_k)\mathbf{B}_2(t_j)u(t_j) + v(t_j)$$

which can be rewritten as

$$x(t_j) = x_o(t_j) + \sum_{k=0}^{j} w(t_j,t_k)u(t_k)$$

$$y(t_j) = x(t_j) + v(t_j)$$

or in matrix form,

$$\begin{vmatrix} \cdot \\ \cdot \\ x(t_{j-1}) \\ x(t_j) \\ x(t_{j+1}) \\ \cdot \end{vmatrix} = \begin{vmatrix} \cdot & 0 & 0 & 0 \\ \cdot & 0 & 0 & 0 \\ \cdot & w(t_{j-1},t_{j-1}) & 0 & 0 \\ \cdot & w(t_j,t_{j-1}) & w(t_j,t_j) & 0 \\ \cdot & w(t_{j+1},t_{j-1}) & w(t_{j+1},t_j) & w(t_{j+1},t_{j+1}) \\ \cdot & \cdot & \cdot & \cdot \end{vmatrix} \begin{vmatrix} \cdot \\ \cdot \\ u(t_{j-1}) \\ u(t_j) \\ u(t_{j+1}) \\ \cdot \end{vmatrix} + \begin{vmatrix} \cdot \\ \cdot \\ x_o(t_{j-1}) \\ x_o(t_j) \\ x_o(t_{j+1}) \\ \cdot \end{vmatrix}$$

$$\begin{vmatrix} \cdot \\ y(t_{j-1}) \\ y(t_j) \\ y(t_{j+1}) \\ \cdot \end{vmatrix} = \begin{vmatrix} \cdot \\ x(t_{j-1}) \\ x(t_j) \\ x(t_{j+1}) \\ \cdot \end{vmatrix} + \begin{vmatrix} \cdot \\ v(t_{j-1}) \\ v(t_j) \\ v(t_{j+1}) \\ \cdot \end{vmatrix}$$

If the disturbance responses $x_o(t_j)$ and the control impulse response $w(t_j,t_k)$ (i.e. the weighting function) are predictable then an open loop control could be found to minimize a performance index of y and u.

1.3 Application to Helicopter Vibration Reduction

For a helicopter in a steady flight condition, the induced vibration can be considered periodic

$$x_o(t_{in+j}) = x_o(t_{in+n+j})$$

where n measurements are made per cycle, which is one quarter of a revolution for a four–bladed rotor when only a single vertical accelerometer is assumed. Thus, if the induced vibration history can be determined for one cycle, it can be predicted to be the same for the next few cycles. If the effect of small blade–lift–controls are negligible after p cycles then the matrix equation becomes

$$\begin{bmatrix} x(t_{in+1}) \\ \vdots \\ x(t_{in+n}) \end{bmatrix} = \mathbf{x}_i \ , \ \begin{bmatrix} u(t_{in+1}) \\ \vdots \\ u(t_{in+n}) \end{bmatrix} = \mathbf{u}_i \ , \ \begin{bmatrix} x_o(t_{in+1}) \\ \vdots \\ x_o(t_{in+n}) \end{bmatrix} = \mathbf{x}_c$$

$$\mathbf{x}_i = \sum_{l=o}^{p} \mathbf{R}_{i-l}\, \mathbf{u}_{i-l} + \mathbf{x}_{o_i} \tag{1.1}$$

where $\mathbf{R}_{i-l}$ is an impulse response matrix relating cycle i–l input to cycle i output.

If the control is nearly constant from one cycle to the next, so that $u(t_{in+j}) \simeq u(t_{in+n+j})$, then the matrix equation can be written for cycle i

$$\mathbf{x}_i = \mathbf{T}_i \mathbf{u}_i + \mathbf{x}_{o_i}$$

$$\mathbf{y}_i = \mathbf{x}_i + \mathbf{v}_i \qquad (1.2)$$

$$\mathbf{T}_i = \sum_{l=o}^{p} \mathbf{R}_{i-l}$$

where $\mathbf{T}_i$ is the "wrapped around" impulse response matrix. Throughout the rest of this report this shall be called simply the impulse response matrix.

The impulse response method thus seeks to find vector $\mathbf{u}_i$ such that a performance index of the vibration vector $\mathbf{x}_i$ is minimized. Note that a more general regulator algorithm can be obtained by using Eq. (1) without the nearly constant control assumption. *Such an algorithm would be more complex, but would permit treatment of transients generated by the control inputs more effectively.*

This development may be generalized such that $\mathbf{u}$ is a vector of m discrete blade inputs evenly distributed throughout the blade azimuth, $\mathbf{y}$ is ameasure of the vector $\mathbf{x}$ of n discrete values of an observable response (typically accelerations) corrupted by noise v. $\mathbf{T}$ is a nxm transfer matrix composed of impulse responses, and $\mathbf{x}_o$ is a n–vect or of discrete values of the uncontrolled vibrations. By the Sampling Theorem, the number of samples per cycle taken of the vibration (n) and used to reconstruct the control signal (m) must be greater than twice the highest harmonic frequency of vibration to be reduced. This rate, however, should be at least four times Nyquist for proper performance. In this study, the highest frequency in the uncontrolled vibration was 8Ω yielding a Nyquist frequency of 16 samples/ revolution, or 4 samples/cycle (one cycle equals one quarter revolution). The rate used here was 8 samples per cycle; therefore m = n = 8 (twice Nyquist).

In the following development the subscript i represents the current cycle count; however, in the interest of simplicity, the indices are only used on expressions which represent relationships between different cycles.

Eq. (1.2) can be rewritten in a more convenient form

$$\mathbf{x} = \boldsymbol{\theta}\mathbf{u} \tag{1.3}$$

where

$$\boldsymbol{\theta} = [\mathbf{x}_0 \mid \mathbf{T}]$$

and

$$\underline{\mathbf{u}} = [1 \mid \mathbf{u}^T]^T$$

Eq. (1.2) is in global model form. It can be written in local model form through simple subtraction

$$(\mathbf{x}_{i+1} = \mathbf{T}_{i+1}\,\mathbf{u}_{i+1} + \mathbf{x}_{0_{i+1}}) - (\mathbf{x}_i = \mathbf{T}_i\,\mathbf{u}_i + \mathbf{x}_{0_i})$$

$$\Delta\mathbf{x}_i = \mathbf{T}_i\,\Delta\mathbf{u}_i \tag{1.4}$$

$$\Delta\mathbf{y}_i = \Delta\mathbf{x}_i + \Delta\mathbf{v}_i$$

where it is assumed that $\mathbf{T}_{i+1} = \mathbf{T}_i$ and $\mathbf{x}_{0_{i+1}} = \mathbf{x}_{0_i}$. Equation (1.4) can be put into the same form as (1.3)

$$\Delta\mathbf{x} = \boldsymbol{\theta}\underline{\mathbf{u}}$$

$$\boldsymbol{\theta} = [\mathbf{T}]$$

$$\underline{\mathbf{u}} = \Delta\mathbf{u}$$

The local model requires less estimation to be performed for the optimal control law. It is also felt by HHC researchers to better represent the globally nonlinear relationship between blade input and fuselage vibration. For small changes in control from a reference blade deflection, the change in control force (and hence counter vibration) produced will be linearly related. However, since the effectiveness of changes in blade deflection varies with blade deflection, this linearity is only valid locally (that is, close to the reference deflection). Equation (1.4) expresses only a locally linear relationship, not a globally linear one as (1.2).

1.4 Circulant Structure of the Impulse Response Matrix

If the plant was not a time varying system, each column of the square impulse response matrix would be an identical permutation of the first column:

$$\mathbf{T} = \begin{bmatrix} T_1 & T_n & T_{n-1} & \cdots & T_2 \\ T_2 & T_1 & T_n & \cdots & T_3 \\ T_3 & T_2 & T_1 & & T_4 \\ \vdots & \vdots & \vdots & & \vdots \\ T_n & T_{n-1} & T_{n-2} & & T_1 \end{bmatrix}$$

Thus, the reaction of an impulse in control at any point during a cycle would result in the same response. A matrix of this form is called a circulant matrix and has many special properties. Of particular interest is that every circulant matrix is diagonalizable by the Fast Fourier ($\mathbf{F}$) and inverse Fast Fourier transform ($\mathbf{F}^*$); therefore if $\mathbf{T}^T = \mathbf{circ}\,(T_1, T_2, \ldots T_n)$

$$\mathbf{T} = \mathbf{F}^* \Lambda \mathbf{F} \qquad \mathbf{F}^* = \mathbf{F}^{-1}$$

$$\Lambda = \mathrm{diag}\,(\lambda_1, \ldots, \lambda_n)$$

and

$$\mathbf{Fx} = \mathbf{F}(\mathbf{F}^{*}\Lambda\mathbf{F})\mathbf{u} + \mathbf{Fx}_{o}$$

$$\tilde{\mathbf{x}} = \Lambda\,\tilde{\mathbf{u}} + \tilde{\mathbf{x}}_{o}$$

where the tilde indicates the FFT of the time sequence vector. Thus, for the stationary plant, the circulant impulse response matrix expresses the spectral response of the transfer function of the plant through its eigenvalues.

If the vertical helicopter impulse response at each blade azimuth can be idealized as the same except for an azimuth dependent magnification factor each column of the impulse response matrix will be a permutation of the first column multiplied by a scalar. The magnification factors are then just an expression of the changing effectiveness of the blade (i.e., coefficient of lift) throughout the azimuth. (The force produced on a blade at any point in the azimuth by an incremental change in blade pitch is a function of the azimuth dependent blade pitch.) This idealization ignores all other azimuth dependent dynamics (such as azimuth dependent blade damping). The author has not seen any research that suggests that the effects of the ignored dynamics will be substantial. Therefore, the helicopter impulse response matrix can be considered decomposable into a circulant matrix, **C**, and a diagonal matrix, **B**:

$$\mathbf{T} = \mathbf{C}\,\mathbf{B}$$

$$\mathbf{C}^{T} = \mathbf{circ}\,(c_1, c_2, \ldots c_n)$$

$$\mathbf{B} = \mathbf{diag}\,(b_1, b_2, \ldots b_n)$$

Note that this decomposition is not necessary for the application of the impulse response method to the helicopter vibration problem. Note also that this

decomposition requires that the control be reconstructed from the same number of samples as are measured per cycle (i.e., m = n). This presents no problem since the control should have a bandwidth as large as that of the uncontrolled vibration.

Applying the circulant diagonalization property to the global model yields

$$\mathbf{x} = \mathbf{C}\,\mathbf{B}\,\mathbf{u} + \mathbf{x}_o \tag{1.5}$$

$$\mathbf{F}\mathbf{x} = \mathbf{F}(\mathbf{F}^{*}\Lambda\mathbf{F})(\mathbf{B}\mathbf{u}) + \mathbf{F}\mathbf{x}_o$$

$$\tilde{\mathbf{x}} = \Lambda(\tilde{\mathbf{B}}\mathbf{u}) + \tilde{\mathbf{x}}_o$$

Thus, each vibration harmonic is the sum of the corresponding uncontrolled vibration harmonic and the corresponding forcing (i.e. $\mathbf{Bu}$) harmonic attenuated and phase shifted by a complex eigenvalue of the circulant matrix. This comes close to relating the impulse response method to the HHC method; HHC relates the harmonics of vibration ($\tilde{\mathbf{x}}$) to harmonics of control ($\tilde{\mathbf{u}}$) via a full matrix. The impulse response matrix formulation can be put into this form:

$$\tilde{\mathbf{x}} = \Lambda(\mathbf{F}\,\mathbf{B}\,\mathbf{F}^{*})\,\mathbf{F}\mathbf{u} + \tilde{\mathbf{x}}_o$$
$$\tilde{\mathbf{x}} = \Lambda\,\mathbf{H}_c\,\tilde{\mathbf{u}} + \tilde{\mathbf{x}}_o$$

$$\mathbf{H}_c = \mathbf{F}\mathbf{B}\mathbf{F}^{*} = \mathbf{circ}\,(h_1, h_2, \ldots h_n)$$

where $\mathbf{H}_c$ is a Hermetic circulant matrix.

1.5 Computer Models of the Plant

The helicopter model employed for the computer simulations to be presented is based upon equation (1.5)

$$\mathbf{x} = \mathbf{C}\,\mathbf{B}\,\mathbf{u} + \mathbf{x}_o$$
$$\mathbf{y} = \mathbf{x} + \mathbf{v}$$

$$\mathbf{C}^T = \mathbf{circ}\,(c_1, c_2, \ldots c_n)$$
$$\mathbf{B} = \mathbf{diag}\,(b_1, b_2, \ldots b_n)$$

where $\mathbf{x}$, $\mathbf{x}_o$, $\mathbf{y}$, $\mathbf{u}$ and $\mathbf{v}$ are 8–vectors, and $\mathbf{C}$ and $\mathbf{B}$ are 8x8 matrices. The 8 elements of $\mathbf{x}_o$ are determined by 4 parameters: a 4Ω amplitude, a 4Ω phase, an 8Ω amplitude, and an 8Ω phase. The 8 non–zero elements of $\mathbf{B}$ are determined by 3 parameters: a bias, a sine function amplitude, and a sine phase. This models the one peak per cycle combined blade lift sensitivity. The elements of the circulant $\mathbf{C}$ matrix are determined by 6 parameters (these determine the first column of the matrix, the wrapped–around impulse response), 3 for each damped vibration mode in the impulse response: an amplitude, a frequency, and a damping. The impulse response is computed for 3 cycles and overlapped to produce the first column of the circulant matrix. Thus, 13 parameters determine all 72 elements of the plant model ($\mathbf{x}_o$, T).

1.6 Kalman Filter Algorithm

To adapt to the changes in the plant, the regulator must incorporate an identification algorithm. The filter developed here parallels that used by Molusis et al. [34], and Bryson and Ho [59]. The $\boldsymbol{\theta}$ matrix varies from cycle to cycle as the

result of disturbances in the atmosphere, flight control input from the pilot, or self induced disturbances, such as interactions between the blade wake and the tail rotor. These variations are modeled by the random walk.

$$\boldsymbol{\theta}_{i+1} = \boldsymbol{\theta}_i + \mathbf{w}_{\theta,i}$$

where $\mathbf{w}_{\theta,i}$ is a matrix of random numbers

$$\mathbf{w}_\theta = [\, \mathbf{w}_X \mid \mathbf{w}_T \,] \qquad \text{global}$$
$$\mathbf{w}_\theta = [\, \mathbf{w}_T \,] \qquad \text{local}$$

Here $\mathbf{w}_X$ is a vector of n random variations in the basic vibration vector $\mathbf{x}_o$ with standard deviation σ_X and $\mathbf{w}_T$ is an nxm matrix of random variations in the transfer matrix T with standard deviation σ_T.

The value of $\boldsymbol{\theta}$ differs from the minimum variance *a posteriori* estimate $\hat{\boldsymbol{\theta}}$ by an error matrix η_θ

$$\eta_\theta = \hat{\boldsymbol{\theta}} - \boldsymbol{\theta} \tag{1.6}$$

$$\eta_\theta = [\, \eta_X \mid \eta_T \,] \qquad \text{global}$$
$$\eta_\theta = [\, \eta_T \,] \qquad \text{local}$$

in which η_X is a vector representing the error in the uncontrolled vibration estimate vector $\hat{\mathbf{x}}_o$, while η_T is a matrix representing the error in the impulse response matrix estimate $\hat{\mathbf{T}}$. The minimum variance *a priori* estimate of $\boldsymbol{\theta}_{i+1}$ is $\bar{\boldsymbol{\theta}}_{i+1}$ and is equal to the previous *a posteriori* estimate $\hat{\boldsymbol{\theta}}_i$, so that

$$\bar{\theta}_{i+1} = \hat{\theta}_i$$

Equations (1.2), (1.3) and (1.6) can now be combined into the state propagation equation which is written as

$$Y = \theta H + \epsilon \tag{1.7}$$

with

$$Y = [\, y \mid \bar{\theta} \,]$$

$$H = [\, \underline{u} \mid I \,] \qquad \underline{u} = [1 \mid u^T]^T \quad \text{global}$$

$$\epsilon = [\, v \mid \zeta_\theta \,] \qquad = \Delta u \quad \text{local}$$

$$\zeta_{\theta,i+1} = \bar{\theta}_{i+1} - \theta_{i+1}$$

$$= \eta_{\theta,i} - w_{\theta,i}$$

1.7 Best Linear Unbiased Prediction

At the end of the ith cycle, several quantities must be updated so that a new control vector u_{i+1} can be found. The *a priori* estimate $\bar{\theta}_{i+1}$ is equal to $\hat{\theta}_i$ which is obtained from the measurement vector y_i of the helicopter dynamics in response to the input of u_i. A linear relationship is assumed

$$\hat{\theta} = Y M$$

The requirement of an unbiased estimate, $E(\hat{\theta}) = \theta$, yields the condition

$$H M = I$$

The best estimate is obtained by minimizing the error covariance matrix, $\mathbf{P}_j$, subject to this condition. The matrix $\mathbf{P}_j$ is defined

$$\mathbf{P}_j = \mathrm{E}\{\eta_{\theta_j}^{\mathrm{T}} \eta_{\theta_j}\}$$

where $\mathrm{E}\{\cdot\}$ is the expected value operator and η_{θ_j} is the j'th row of the estimate error matrix. This minimization yields the Kalman filter algorithm for the estimate of j'th row of $\boldsymbol{\theta}$

$$\begin{aligned} \overline{\mathbf{P}}_{j_{i+1}} &= \overline{\mathbf{P}}_{j_i} - \overline{\mathbf{P}}_{j_i} \underline{\mathbf{u}}_i \mathbf{K}_{j_i}^{\mathrm{T}} + \mathbf{W}_j \\ \overline{\theta}_{j_{i+1}} &= \hat{\theta}_{j_i} = \overline{\theta}_{j_i} + (\mathbf{y}_{j_i} - \overline{\theta}_{j_i} \underline{\mathbf{u}}_i) \mathbf{K}_{j_i}^{\mathrm{T}} \end{aligned} \tag{1.8}$$

Here, $\mathbf{K}_{j_i}$ is the Kalman gain vector

$$\mathbf{K}_{j_i} = \overline{\mathbf{P}}_{j_i} \underline{\mathbf{u}}_i / (\underline{\mathbf{u}}_i^{\mathrm{T}} \overline{\mathbf{P}}_{j_i} \underline{\mathbf{u}}_i + \mathrm{V}_j)$$

while

$$\mathrm{V}_j = \mathrm{E}\{\mathbf{v}_j^{\mathrm{T}} \mathbf{v}_j\} = \sigma_{\mathrm{v}}^2 \qquad \text{global}$$

$$= 2\,\sigma_{\mathrm{v}}^2 \qquad \text{local}$$

$$\mathbf{W}_j = \mathrm{E}\{(\theta_{j_{i+1}} - \theta_{j_i})^{\mathrm{T}} (\theta_{j_{i+1}} - \theta_{j_i})\} = \mathbf{diag}\{\sigma_{\mathrm{x}}^2, \sigma_{\mathrm{T}}^2, \ldots, \sigma_{\mathrm{T}}^2\} \qquad \text{global}$$

$$= \mathbf{diag}\{\sigma_{\mathrm{T}}^2, \sigma_{\mathrm{T}}^2, \ldots, \sigma_{\mathrm{T}}^2\} \qquad \text{local}$$

and $\overline{P}_j$ is the *a priori* estimate error covariance matrix

$$\overline{P}_j = E\{(\overline{\theta}_j - \theta_j)^T (\overline{\theta}_j - \theta_j)\}$$

Therefore, for the estimation of each row of θ, an nxn matrix, $\overline{P}_j$, must be updated (and stored) and an nx1 vector, K_j, must be computed. These are dependent on the noise covariance on the j'th measurement, V_j, and the process noise covariance matrix for the j'th row of θ, W_j. There is no reason to assume in advance that these quantities will be different for different rows; and, considerable computational advantage can be achieved by assuming them equivalent. In this case, the individual row equations (1.8) can be collated into a single matrix update equation for the estimate and a single equation for the covariance matrix

$$\overline{\theta}_{i+1} = \overline{\theta}_i + (y_i - \overline{\theta}_i \underline{u}_i) K_i^T \tag{1.9}$$

$$\overline{P}_{i+1} = \overline{P}_i - \overline{P}_i \underline{u}_i K_i^T + W$$

$$K_i = \overline{P}_i \underline{u}_i / (\underline{u}_i^T \overline{P}_i \underline{u}_i + V)$$

$$V = \sigma_v^2 \qquad \text{global}$$
$$= 2\,\sigma_v^2 \qquad \text{local}$$
$$W = \mathbf{diag}\{\sigma_x^2, \sigma_T^2, \ldots, \sigma_T^2\} \qquad \text{global}$$
$$= \mathbf{diag}\{\sigma_T^2, \ldots, \sigma_T^2\} \qquad \text{local}$$

This reduces the computational burden n–fold. While in a typical flight, the actual variation in each row of $\boldsymbol{\theta}$ will be different, it is difficult to prescribe the row process noise covariance matrices in advance. Therefore, this assumption is also practical. This will result in a degradation in the estimation performance in comparison to the optimally tuned individual row filters.

The Kalman filter algorithm (1.9) recursively updates a measure of its uncertainty, $\overline{\mathbf{P}}$, and the *a priori* estimate, $\overline{\boldsymbol{\theta}}$. The change in the estimate of i'th column produced by the update is the residual vector $(\mathbf{y}_i - \overline{\boldsymbol{\theta}}_i \underline{\mathbf{u}}_i)$ multiplied by the j'th element of the Kalman gain vector $\mathbf{K}_i$. The residual vector is the only expression of the error in the estimate available to the filter; it is the measured output vector less the expected output vector based upon the estimate. The Kalman gain vector expresses the usefulness of this information to the updating of each column of the estimate matrix. The larger the magnitudes of the elements of the Kalman gain vector the greater the change in the estimate will be and the greater the reduction in the covariance ellipsoid via the $\overline{\mathbf{P}}_i \underline{\mathbf{u}}_i \mathbf{K}_i^T$ term. Quite simply, if the residual information is very useful, then the expected error of a new estimate based on it should decrease from the previous estimate. (Note that the usefulness of the residual is inversely proportional to the expected measurement noise covariance, V.) Of course any change in the the value after the measurement is taken will increase the estimate's inaccuracy, hence the addition of the process noise term, **W**, to the previous covariance.

If the plant is stationary and the measurement noise is small, the Kalman filter estimates will converge to the true values in approximately m+1, for the global model, or m, for the local model, steps. Also, if the plant is stationary the Kalman filter algorithm is stable if the covariance remain bounded. The greatest problem in employing the Kalman filter is the extensive tuning (that is adjustment

of the measurement noise and process noise covariances) required for near–optimal performance. In this study, it is assumed that the measurement noise standard deviation will be known very accurately; therefore, tuning refers here to the adjustment of the process noise terms, which are the filters representation of the true covariances, σ_x^2 and σ_T^2.

1.8 Kalman Filter Covariance Stability

The Kalman filter equations (1.9) can become unstable via growth in the covariance ellipsoid if the control fails to yield information along axes of the parameter space. For example, if all the elements of the control vector are always zero except the k'th which is always one, then

$$\bar{P}_{i+1} = \bar{P}_i + W + \frac{\bar{P}_{k_i}\,\bar{P}_{k_i}^T}{\bar{P}_{kk_i} + V} \tag{1.10}$$

where $\bar{P}_k$ is the k'th column of $\bar{P}$ and $\bar{P}_{kk}$ is the k'th element of $\bar{P}_k$. Then, equations for the elements of $\bar{P}$ can be written:

$$\begin{aligned}
\bar{P}_{11_{i+1}} &= \bar{P}_{11_i} + W_{11} - \bar{P}_{1k_i}^2/(\bar{P}_{kk_i} + V) \\
\bar{P}_{kk_{i+1}} &= \bar{P}_{kk_i} + W_{kk} - \bar{P}_{kk_i}^2/(\bar{P}_{kk_i} + V) \\
\bar{P}_{1k_{i+1}} &= \bar{P}_{1k_i} - \bar{P}_{1k_i}\,\bar{P}_{kk_i}/(\bar{P}_{kk_i} + V)
\end{aligned} \tag{1.11}$$

The second equation converges to the stable root

$$\bar{P}_{kk_\infty} = \frac{1}{2}\left[W_{kk} + \sqrt{W_{kk}^2 + 4W_{kk}V}\right] > 0$$

As this occurs, the last equation uniformly converges as

$$\bar{P}_{1k_{i+1}} = \bar{P}_{1k_i}\left(1 - \frac{\bar{P}_{kk_\infty}}{\bar{P}_{kk_\infty} + V}\right)$$

to zero ($\bar{P}_{1k_\infty} = 0$) since $0 < (1 - \bar{P}_{kk_\infty}(\bar{P}_{kk_\infty} + V)^{-1}) < 1$. Therefore, the first equation becomes

$$\bar{P}_{11_{i+1}} = \bar{P}_{11_i} + W_{11} - \bar{P}_{1k_\infty}^2/(\bar{P}_{kk_\infty} + V)$$

or

$$\bar{P}_{11_{i+1}} = \bar{P}_{11_i} + W_{11} \tag{1.12}$$

as the second and third equations approach their roots. It is easy to see from (1.12) that this covariance will go unstable under this control. Furthermore, it can be shown in the same manner that all $\bar{P}_{jj}$, $j \neq k$, will go unstable under this control. The covariance ellipsoid is growing along all axes except the k'th along which the filter is receiving information. This may seem like an unusual case; after all, the control is not likely to be zero in every element but one. However, if the control is a constant vector, then through an orthogonal transform **L** we can rotate the axis system such that

$$u_L = Lu = [\,0\ 0\ \ldots\ 0\ 1\ 0\ \ldots\ 0\,]^T$$

(In general, the magnitude of the constant control can always be one if the measurement and process noises are also scaled.) Then, by applying the transform to the covariance equation,

$$L\,\bar{P}_{i+1}\,L^T = L\,\bar{P}_i\,L^T + L\,W\,L^T - \frac{L\,\bar{P}\,L^T(Lu)(u^TL^T)L\,P\,L^T}{(u^TL^T)(L\,P\,L^T)(Lu) + V}$$

(which is geometrically equivalent to rotating the covariance ellipsoid in the n–space) and the substitution

$$\bar{P}_L = L\,\bar{P}\,L^T \qquad\qquad u_L = Lu$$

the recursive equation for $\bar{P}$ is converted to the form of (1.10).

An examination of the case where one element of the control is zero (and the others may vary) is useful. The covariance update equation (1.9) can be partitioned as

$$\left[\begin{array}{c|c} \bar{P}_a & \bar{P}_b \\ \hline \bar{P}_b^T & \bar{P}_{nn} \end{array}\right]_{i+1} = \left[\begin{array}{c|c} \bar{P}_a & \bar{P}_b \\ \hline \bar{P}_b^T & \bar{P}_{nn} \end{array}\right]_i + \left[\begin{array}{c|c} W_a & 0 \\ \hline 0 & W_{nn} \end{array}\right]$$

$$- \frac{\left[\begin{array}{c|c} \bar{P}_a & \bar{P}_b \\ \hline \bar{P}_b^T & \bar{P}_{nn} \end{array}\right]_i \left[\begin{array}{c} u_a \\ \hline 0 \end{array}\right]_i \left[\begin{array}{c|c} u_a^T & 0 \end{array}\right]_i \left[\begin{array}{c|c} \bar{P}_a & \bar{P}_b \\ \hline \bar{P}_b^T & \bar{P}_{nn} \end{array}\right]_i}{u_{a_i}^T\,\bar{P}_{a_i}\,u_{a_i} + V}$$

to yield

$$\bar{P}_{a_{i+1}} = \bar{P}_{a_i} + W_a - \frac{\bar{P}_{a_i} u_{a_i} u_{a_i}^T \bar{P}_{a_i}}{u_{a_i}^T \bar{P}_{a_i} u_{a_i} + V}$$

$$\bar{P}_{b_{i+1}} = \left[I - \frac{(\bar{P}_{a_i} u_{a_i} u_{a_i}^T)}{u_{a_i}^T \bar{P}_{a_i} u_{a_i} + V} \right] \bar{P}_{b_i} \qquad (1.13)$$

$$\bar{P}_{nn_{i+1}} = \bar{P}_{nn_i} + W_{nn} - \frac{(u_{a_i}^T \bar{P}_{b_j})^2}{u_{a_i}^T \bar{P}_{a_i} u_{a_i} + V}$$

The bracketed matrix in the second equation of (1.13) has eigenvalues

$$\lambda_1 = 1 - \frac{u_{a_i}^T \bar{P}_{a_i} u_{a_i}}{u_{a_i}^T \bar{P}_{a_i} u_{a_i} + V} > 0$$

$$\lambda_j = 1 \qquad j \neq 1$$

Since all the eigenvalues are less than or equal to one, any norm of $\bar{P}_{b_{i+1}}$ cannot increase from i to i+1 Therefore, over time the magnitude of the vector $\bar{P}_b$ will decrease; as this occurs, the last equation will increasingly resemble

$$\bar{P}_{nn_{i+1}} = \bar{P}_{nn_i} + W_{nn}$$

Thus, with one element of the control always zero, one axis of the covariance ellipsoid will tend to grow unbounded. This is geometrically equivalent to the case where the control is constrained to lie in a space orthogonal to a fixed vector; that is, through a coordinate transformation one axis of the basis can be aligned with the fixed vector yielding a representation of the control with the corresponding element fixed equal to zero. Thus, if the control is constrained to have zero mean, then one eigenvector of the covariance ellipsoid will grow unbounded. This growth in covariance represents the increasing uncertainty in the filter over the estimate of $\overline{\mathbf{T}}$. If every element of $\mathbf{T}$ were to increase by the same constant, then this change would be unrepresented in the residual when the control is constrained to have zero mean. While this behavior is exceedingly unlikely, the covariance equations instability represents the chance of it occurring given the random walk description of the plant model.

These arguments can be generalized to say that the number of bounded eigenvalues as the recursion approaches infinity is equal to the minimum rank of the control matrix

$$\mathbf{U}_\ell = \left[\mathbf{u}_\ell \,\middle|\, \mathbf{u}_{\ell+1} \,\middle|\, \cdots \,\middle|\, \mathbf{u}_{\ell+1} \,\middle|\, \cdots \right] \quad , 0 < \ell < \infty \tag{1.14}$$

over finite ℓ. This behavior can be seen in Figures 1.1 through 1.3 which show the growth in the eigenvalues of a 9x9 covariance matrix under rank 9, 8, and 7 control. (The control moves mod p through a set of p unit vectors.) Note that the number of 'bounded' eigenvalues is that predicted by the minimum rank of (1.14).

Since in any sustained flight condition the optimal control may be almost constant, it is likely that in operation an on–board Kalman filter will often produce

uncertainties much larger than the actual estimate errors. This would especially degrade the performance of cautious regulators. This covariance growth can be prevented through a variety of means, such as process noise turn–off, random probing control and covariance trace bounding.

1.9 Weighted Least Squares Algorithm

The moving batch least squares filter algorithm finds the estimate that minimizes the sum of the past ℓ residuals squared. If the measurement noise was zero and the plant was stationary, this method would produce perfect estimates with any batch size greater than or equal to the minimum of m+1 (global) or m (local). If the plant is slowly changing, the estimate accuracy is increased by weighting the most recent residual squares greater (if the batch size is not equal to the minimum). The derivation of the weighted least squares (WLS) algorithm is straightforward. Define the collections of ℓ measurement vectors and control vectors (where the subscript B stands for batch) as

$$Y_B = \left[\, y_{i-1} \, \middle| \, y_{i-2} \, \middle| \, \cdots \, \middle| \, y_{i-\ell} \, \right] \qquad U_B = \left[\, \underline{u}_{i-1} \, \middle| \, \underline{u}_{i-2} \, \middle| \, \cdots \, \middle| \, \underline{u}_{i-\ell} \, \right]$$

Then the collection of residuals is

$$[\, Y_B - \overline{\theta}_i U_B \,]$$

where $\overline{\theta}_i$ is a prediction of θ_i. A performance function that is the weighted sum of the ℓ residual vectors,

$$J = \sum_{k=1}^{\ell} (y_{i-k} - \bar{\theta}_i u_{i-k})^T \phi_k (y_{i-k} - \bar{\theta}_i u_{i-k})$$

where ϕ_k are the weights, can be shown equivalent to the performance function

$$J = \text{trace} (W_B [Y_B - \bar{\theta}_i U_B]^T [Y_B - \bar{\theta}_i U_B])$$

$$W_B = \text{diag} (\phi_1, \phi_2, ..., \phi_\ell)$$

Since arguments within the trace parentheses can be permuted without affecting its value, this can be re–arranged to

$$J = \text{trace} ([Y_B - \bar{\theta}_i U_b] \; W_B [Y_B - \bar{\theta}_i U_B]^T)$$

It is easy to show that when the first variation is taken of J, the variations in the right hand side may be taken within the trace parentheses yielding

$$\partial J = \text{trace} (\partial \bar{\theta}_i \{-U_B W_B Y_B^T + U_B W_B U_B^T \bar{\theta}_i^T\}$$

$$+ \{ -Y_B W_B U_B^T + \bar{\theta}_i U_B W_B U_B^T\} \partial \bar{\theta}_i^T)$$

Setting ∂J equal to zero yields

$$\bar{\theta}_i U_B W_B U_B^T = Y_B W_B U_B^T$$

Therefore, the weighted least squares estimate of θ_i is

$$\bar{\theta}_{WLS_i} = Y_B W_B U_B^T (U_B W_B U_B^T)^{-1} \tag{1.15}$$

This same result may alternately be shown by minimizing the n performance functions

$$J_k = (Y_{B_k} - \bar{\theta}_{k_i} U_B) \; W_B \, (Y_{B_k} - \bar{\theta}_{k_i} U_B)^T$$

with respect to $\bar{\theta}_{k_i}$, where the k subscript on Y_B and $\bar{\theta}_i$ refers to the k'th row of the matrix. This yields the WLS estimate of θ_{k_i}

$$(\bar{\theta}_{k_i})_{WLS} = Y_{B_k} W_B U_B^T (U_B W_B U_B)^{-1}$$

The n estimate rows can then be collected together to yield (1.15).

Note that the control batch matrix U_B must have rank m+1 for the global model and rank m for the local if equation (1.15) is to be used. Without constraints, this is highly likely although the matrix may still be poorly conditioned (especially in steady flight conditions when the control may change very little). Care must be taken to minimize numerical error in these computations. (A special IMSL routine was used in this study's simulations.) Increasing batch size will, in most cases, result in a better conditioned matrix for inversion. For a stationary plant, an increase in batch size should produce greater noise suppression and better estimation. If the plant is varying quickly, the estimates will lag the true values

more when the larger batch sizes are used. Therefore, generally, a batch size slightly larger than the minimum will estimate with the most accuracy, a trade–off between noise suppression and filter sensitivity.

The advantages of the WLS algorithm are that it is always stable (since it is non–recursive) and it needs no 'tuning' except for the weighting parameters. For the research conducted here, the weighting scheme employed by Jacklin and Franklin and Powell is used [58]:

$$\phi_k = (\alpha)^{k-1}$$

where α is a fixed constant between zero exclusive and one inclusive. One disadvantage of the method for this application, is that a zero mean control batch can never be of rank m+1 for global or rank m for local. This may be remedied by adding a small random noise to the control, in effect, breaking the constraint deterministically, but not stochastically.

1.10 Circulant Form and Estimation

If the true plant has the input/output relationship of (1.5),

$$\mathbf{x} = \mathbf{C}\,\mathbf{B}\,\mathbf{u} + \mathbf{x_o}$$
$$\mathbf{y} = \mathbf{x} + \mathbf{v}$$

$$\mathbf{C}^T = \mathbf{circ}\,(c_1, c_2, \ldots c_n)$$
$$\mathbf{B} = \mathbf{diag}\,(b_1, b_2, \ldots b_n)$$

then only 3n parameters entirely describe the plant as opposed to $n^2 + n$. Therefore, for a stationary plant with zero measurement noise, the unknown parameters can be solved for with only 3 measurement vectors taken, as opposed to n+1. It is easy to see that if the plant is described in this form the estimates of the impulse response matrix can track quick changes in the plant (such as produced during maneuvers) with much greater accuracy. Unfortunately, however, since the parameters to be estimated are multiplied, the filtering problem is now nonlinear. Therefore, either a linearization needs to be performed so that an extended Kalman filter (EKF) can be used, or a full scale nonlinear filter must be derived. This second course of action is exceedingly complex. The first method's derivation is a reasonably simple task, but the stability of the resultant filter is unpredictable. Also, if the parameters of **C** and **B** change quickly, the linearization will be invalid and the filter will diverge. The tuning of the EKF will also be of greater complexity and the filter will be computationally more burdensome as well. Nevertheless, if EKF stability for this model could be shown in operation, the increased tracking ability of this filter would be of sufficient worth to merit its use.

One method of incorporating into the estimation the knowledge that the impulse response matrix is of **CB** form without linearized or nonlinear filtering is to correct the Kalman filter or WLS estimate so that it is of the same form. This process is referred to in this study as *circulant estimation enhancement*. This may be done by a variety of ad hoc methods. The method used here "unwinds" the estimate matrix through permutations of each column, determines the B diagonal elements by averaging the ratios of each column with the first column element by element, and then averages over the columns to determine the impulse response. The algorithm is:

$$(\overline{T}_K)_{CEE} = \frac{1}{n} \sum_{j=1}^{n} \Pi^{j-k}\, \overline{T}_j \frac{(\overline{T}_1^{\div}\ \Pi^{k-1}\ \overline{T}_k)}{(\overline{T}_1^{\div}\ \Pi^{j-1}\ \overline{T}_j)}$$

$$\Pi = \begin{bmatrix} 0 & 1 & 0 & 0 & \cdots & 0 \\ 0 & 0 & 1 & 0 & \cdots & 0 \\ \vdots & \vdots & \ddots & \ddots & \ddots & 0 \\ 0 & \vdots & & \ddots & \ddots & 1 \\ 1 & 0 & \cdots & \cdots & \cdots & 0 \end{bmatrix}$$

$$\overline{T}_1^{\div} = [(1/\overline{T}_{11}), (1/\overline{T}_{21}), \ldots (1/\overline{T}_{n1})]$$

$$\overline{T}_1 = [\overline{T}_{11}, \overline{T}_{21}, \ldots \overline{T}_{n1}]^T$$

where $\overline{T}_j$ is the j'th column of $\overline{T}$ and $(\overline{T}_k)_{CEE}$ is the k'th column of the corrected estimate. It is important to emphasize here that if the estimate errors of $\overline{T}$ are large, the above procedure will result in an even poorer estimate. This algorithm coupled with a Kalman filter (which would use $\overline{T}_{CEE}$ in the next recursion) can therefore produce true filter instability. Note that many products of matrices **CB** lie near $\overline{T}$ (infinite if a magnitude constraint is not placed on the first column of **C** or the trace of **B**). An optimal solution for **C** and **B** (2n parameters) that minimize a measure of the error matrix [**CB** – $\overline{T}$] could be computed but this would require solving 2n nonlinear equations after every update. (Another CEE algorithm based on unit vectors of each column was initially tested but was found to be much more sensitive than the above algorithm.)

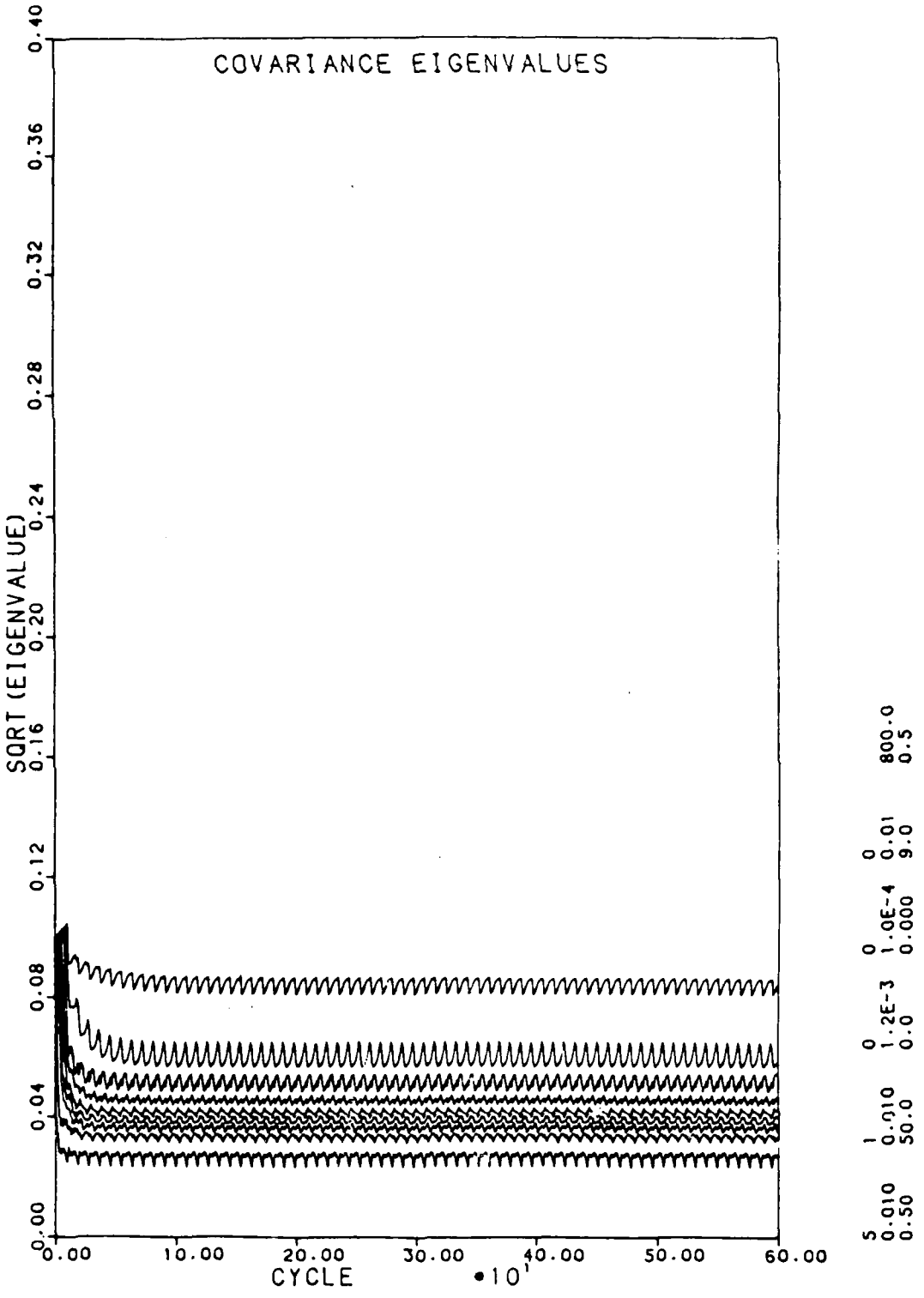

Figure 1.1 Square roots of the 9x9 Covariance matrix eigenvalues with rank 9 deterministic control

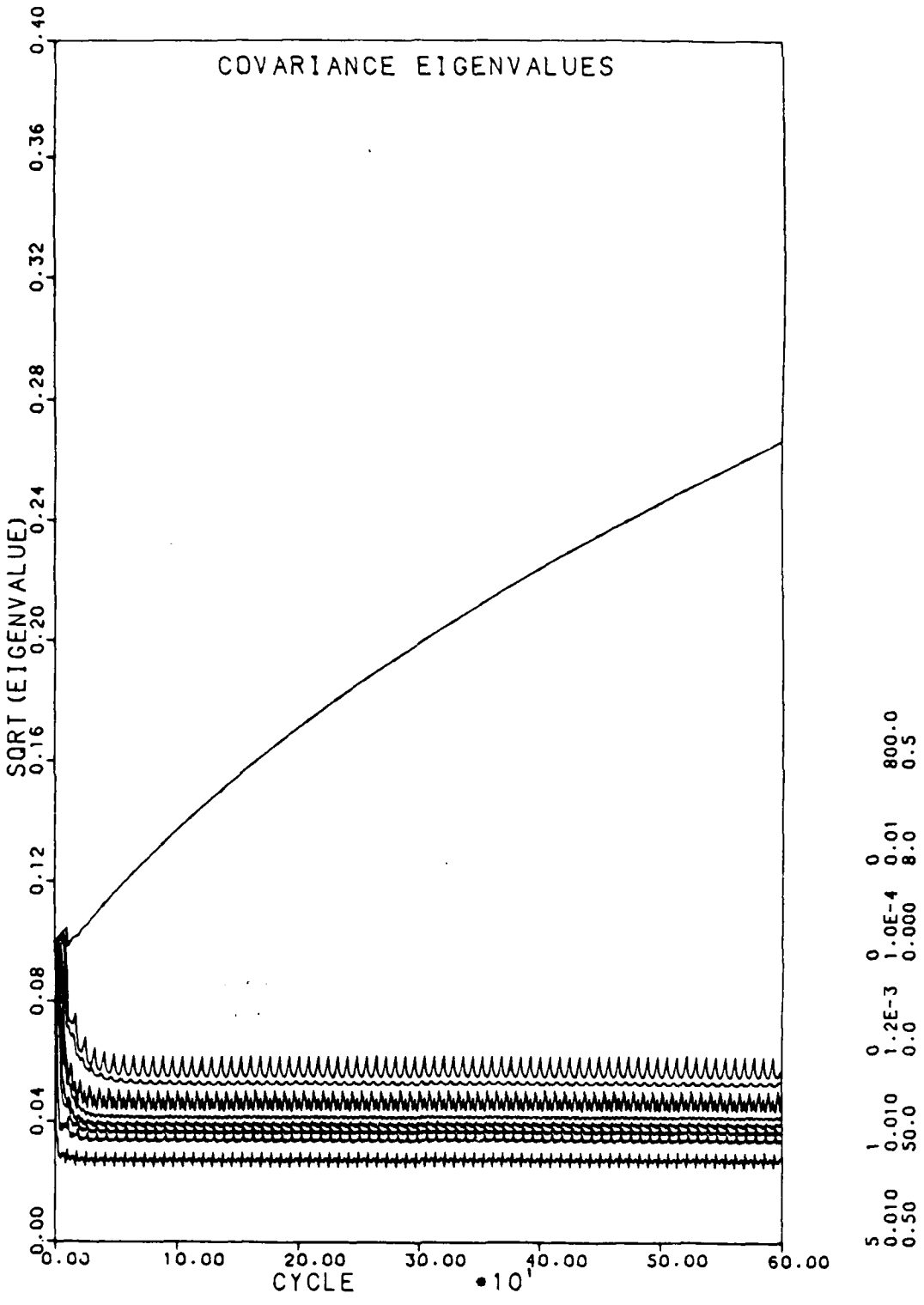

Figure 1.2 Square roots of the 9x9 Covariance matrix eigenvalues with rank 8 deterministic control

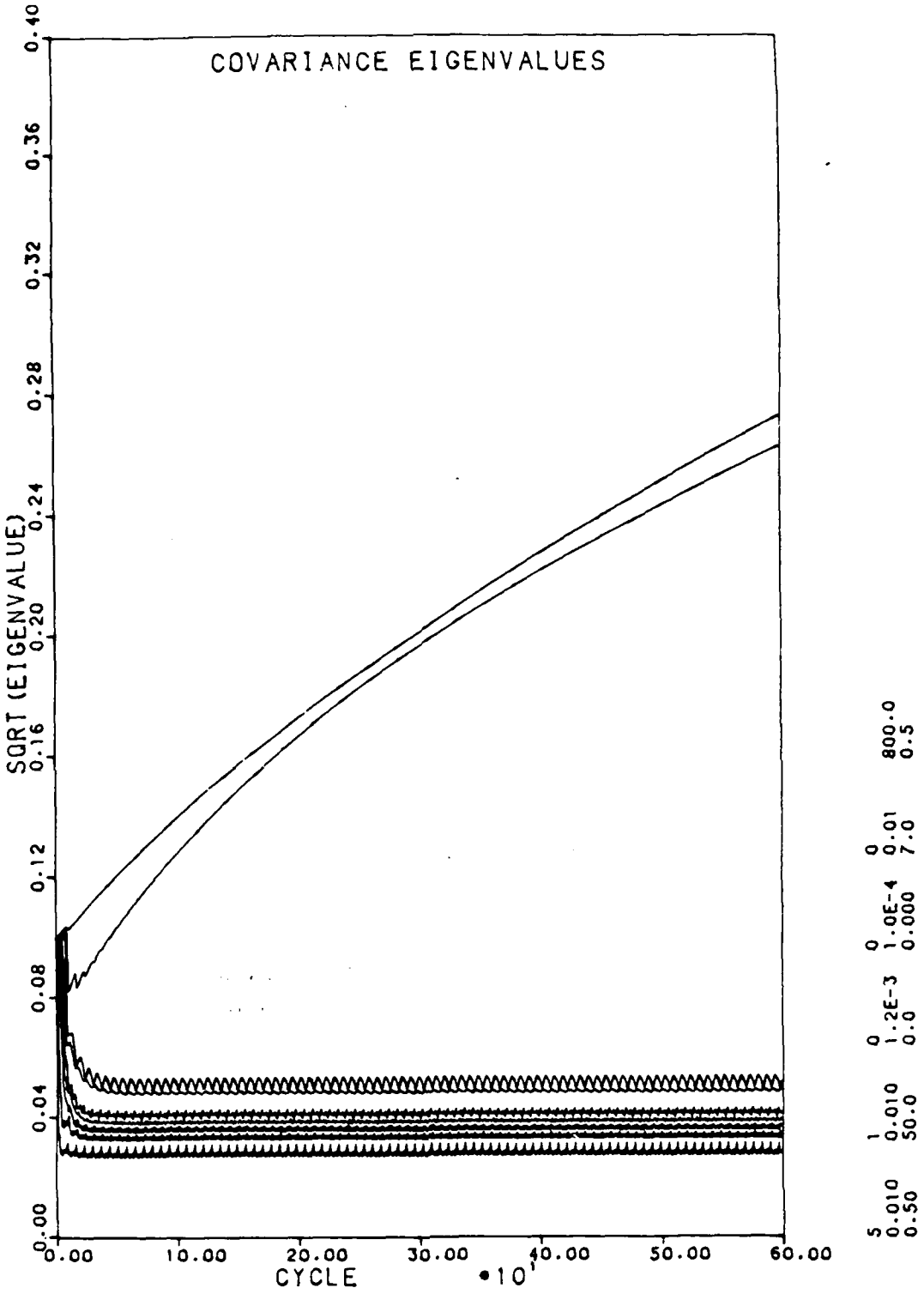

Figure 1.3 Square roots of the 9x9 Covariance matrix eigenvalues with rank 7 deterministic control

CHAPTER TWO: CONTROLLERS

2.1 Introduction

With the plant identified, a control signal can be fashioned so as to reduce the vibration. Typically, optimal control theory is used to determine a control law that minimizes a performance index. The control law is just the functional relationship between the control that minimizes the performance index, and the plant parameters, filter parameters, plant estimates, and measured quantities that comprise the information state. Usually, for a discrete plant model of the type employed here, the performance index is a quadratic of the output vector plus additional terms that are functions of the input vector or estimate covariance. These additional terms are quadratics attempting to discourage certain behaviors or constraints prohibiting them. The performance index may be a multistep or single step formulation of all these terms (output vector quadratic, input vector functions, covariance functions, and constraints). Depending upon whether the performance function is formulated in terms of the expected value operator or the identity operator, is single step or multi–step, and on what terms are included, certainty equivalent, cautious, dual, or sub–optimal dual control laws will result from the minimization of the performance function.

Three additional terms are added to the vibration quadratic to form the performance function for use in this study. They are a control quadratic term, $(\mathbf{u}^T\mathbf{u})r_1$, a control–rate quadratic term $(\Delta\mathbf{u}^T\Delta\mathbf{u})r_2$, and an undesirable control mode constraint, $\mathbf{u}^T\Psi\Lambda$. Here, $\mathbf{u}$ is the mx1 control vector, $\Delta\mathbf{u}$ is the control change vector, r_1 and r_2 are weighting factors, Ψ is an mxℓ matrix whose columns represent the ℓ undesirable control modes, and Λ is a ℓ–vector of undetermined Lagrangian multipliers. The constraint is used to prevent the vibration reduction

control from initiating rigid body motion. For this study, the plant model has been formulated in terms of a quarter revolution per cycle in vertical vibration only. Therefore, the only rigid body mode of concern is vertical, and the only constraint is that the control has zero mean. The control quadratic term is included to encourage the choice of low magnitude control, since the accuracy of the model is degraded by large blade angles of attack. (This would also result in higher blade loads, and possibly actuation difficulties). The control–rate quadratic is included so as to limit actuator power requirements, increase the accuracy of the filter model, and aid in vibration reduction through control noise filtering. The weighting parameters allow the relative importance of these quadratic terms to be adjusted.

One interesting modification to the performance function, which is not included in this research, is the introduction of an 'internal' control rate quadratic to limit the control variation within a cycle. This would be useful in discouraging control vectors which required large control changes within a cycle and therefore result in high actuator power requirements. This can be formulated by including a quadratic of the differences between each element of the control vector and its neighbors:

$$(u^T G u)\, r_3 \quad \text{with } G = \begin{bmatrix} 2 & -1 & 0 & \cdots & 0 & -1 \\ -1 & 2 & -1 & 0 & \cdots & 0 \\ 0 & -1 & 2 & -1 & & 0 \\ \vdots & 0 & -1 & 2 & \ddots & \vdots \\ 0 & & \ddots & \ddots & \ddots & -1 \\ -1 & 0 & \cdots & 0 & -1 & 2 \end{bmatrix}$$

This may be necessary when the impulse response method is wind tunnel tested, especially if a large bandwidth of vibrations is to be reduced.

In the investigation for this project, the performance function was written as a single step of the quadratic terms and the constraint. Dual control laws are very

difficult to formulate and have not justified their complexity sufficiently in previous studies to merit inclusion in this preliminary investigation of impulse response method control. They do have many interesting properties, however, and should be investigated in further studies.

2.2 Global Certainty Equivalent Control Law

The deterministic performance function,

$$J = x^T x + (u^T u) r_1 + (\Delta u^T \Delta u) r_2 + u^T \Psi \Lambda + \Lambda^T \Psi^T u \tag{2.1}$$

where all quantities without subscripts are for cycle i+1, yields the global certainty equivalent control law through substitution of the global model equation

$$x = T u + x_o \tag{2.2}$$

and control rate vector definition

$$\Delta u \equiv u - u_i \tag{2.3}$$

where u_i is the cycle i control, into (2.1):

$$\begin{aligned} J = {} & x_o^T x_o + u^T T^T x_o + u^T T^T T u + x_o^T T u + u^T u (r_1 + r_2) \\ & + u_i^T u_i \, r_2 - u^T u_i r_2 - u^T u \, r_2 + u^T \Psi \Lambda + \Lambda^T \Psi^T u \end{aligned} \tag{2.4}$$

Taking the first variation of the performance function yields

$$\begin{aligned} \partial J = {} & \partial u^T \{T^T x_o + T^T T u + u(r_1 + r_2) - u_i \, r_2 + \Psi \Lambda\} \\ & + \partial \Lambda^T \{\Psi^T u\} + \{u^T \Psi\} \partial \Lambda \\ & + \{u^T T^T T + x_o^T T + u^T (r_1 + r_2) - u_i^T \, r_2 + \Lambda^T \Psi\} \end{aligned} \tag{2.5}$$

where the bracketed terms must equal zero by the calculus of variations when ∂J is set to zero. Therefore,

$$[T^T T + I(r_1 + r_2)]\, u + T^T x_o - u_i\, r_2 + \Psi\Lambda = 0 \tag{2.6}$$

By linear algebraic manipulation the control law is found:

$$Z \equiv [T^T T + I\,(r_1 + r_2)]$$

$$u = -\,Z^{-1}\,[T^T x_o - u_i\, r_2 + \Psi\Lambda]$$

$$\Psi^T u = 0 = -\Psi^T Z^{-1}\,[T^T x_o - u_i r_2] - \Psi^T Z^{-1}\Psi\Lambda$$

$$\Lambda = -[\Psi^T Z^{-1}\Psi]^{-1}\,\Psi^T Z^{-1}\,[T^T x_o - u_i r_2]$$

$$u = -Z^{-1}[T^T x_o - u_i\, r_2] + Z^{-1}\,\Psi[\Psi^T Z^{-1}\Psi]^{-1}\,\Psi^T Z^{-1}\,[T^T x_o - u_i\, r_2]$$

$$u = \{Z^{-1}\Psi[\Psi^T Z^{-1}\Psi]^{-1}\Psi^T - I\}\, Z^{-1}X \tag{2.7}$$

where

$$Z = [T^T T + I(r_1 + r_2)] \tag{2.8}$$

$$X = [T^T x_o - u_i\, r_2] \tag{2.9}$$

Because of the similarities between the performance functions used in this study, all the optimal control laws have the form of (2.7) while the definitions of (2.8) and (2.9) for the matrix Z and the vector X are different in each case. (This form

results from the orthogonality constraint term; the undesired control modes are eliminated through the use of a Householder transform.) The true plant values $\mathbf{x}_0$ and $\mathbf{T}$ are unknown, therefore the filter must supply estimates to be used in (2.8) and (2.9). But, since the control for cycle i+1, $\mathbf{u}$, is computed during cycle i and the output y_i is not available until the end of cycle i, new *a posteriori* estimates of the parameters are unavailable for control computation. The control, therefore, must use the cycle i *a priori* estimates, $\bar{\mathbf{x}}_{0_i}$ and $\bar{\mathbf{T}}_i$ in (2.8) and (2.9). Thus, the control derived

$$\mathbf{u}_{i+1} = \{Z^{-1}\Psi[\Psi^T Z^{-1}\Psi]^{-1}\ \Psi^T - I\}\ Z^{-1}X$$

$$\mathbf{Z} = [\bar{\mathbf{T}}_i^T\ \bar{\mathbf{T}}_i + \mathbf{I}\ (r_1 + r_2)] \tag{2.10}$$

$$\mathbf{X} = [\bar{\mathbf{T}}_i^T\ \bar{\mathbf{x}}_{0_i} - \mathbf{u}_i\ r_2] \tag{2.11}$$

is optimal with respect to an information state which is one cycle old. The resulting flow of measurements, estimates, and controls between the plant, estimator, and controller is shown in Figure 2.1.

2.3 Local Certainty Equivalent Control Law

By substituting in the local model relations

$$\begin{aligned} \Delta x &= T\ \Delta u \quad . \quad \Delta x = x - x_i \\ y &= x + v \qquad \Delta u = u - u_i \end{aligned} \tag{2.12}$$

for $\mathbf{x}$ and $\mathbf{u}$ the performance function of (2.1) becomes

$$J = \Delta u^T T^T T\, \Delta u + \Delta u^T T^T x_i + x_i^T T\, \Delta u + x_i^T x_i + u_i^T u_i\, r_1 + \Delta u^T u_i\, r_1 + u_i^T \Delta u\, r_1 + (r_1 + r_2)\, \Delta u^T \Delta u + \Delta u^T \Psi \Lambda + \Lambda^T \Psi^T \Delta u \tag{2.13}$$

After taking the first variation of J and setting it equal to zero, the local analogues to (2.6) are obtained:

$$[T^T T + I\,(r_1 + r_2)]\, \Delta u + T^T x_i + u_i\, r_1 + \Psi \Lambda = 0$$
$$\Psi^T \Delta u = 0 \tag{2.14}$$

Here, if we set

$$Z = [T^T T + I\,(r_1 + r_2)] \tag{2.15}$$

$$X = [T^T x_i + u_i\, r_1] \tag{2.16}$$

algebraic manipulation yields the same form as (2.7)

$$\Delta u_{i+1} = \{Z^{-1} \Psi\, [\Psi^T Z^{-1} \Psi]^{-1} \Psi^T - I\}\, Z^{-1} X$$

Once again, to obtain the quantities to use in (2.15) and (2.16) we must use the cycle i *a priori* estimate $\overline{T}_i$. Furthermore, since the best estimate of x_i, y_i, is unavailable in cycle i to compute the cycle i+1 control, the relation

$$x_i = x_{i-1} + T_i\, \Delta u_i \tag{2.17}$$

must be used. This yields the local certainty equivalent optimal control law:

$$u_{i+1} = u_i + \{Z^{-1}\,\Psi[\Psi^T Z^{-1}\Psi]^{-1}\,\Psi^T - I\}\,Z^{-1}\,X \tag{2.18}$$

$$Z = [\overline{T}_i^T\,\overline{T}_i + I\,(r_1 + r_2)] \tag{2.19}$$

$$X = [\overline{T}_i^T\,y_{i-1} + \overline{T}_i^T\,\overline{T}_i\,\Delta u_i + u_i\,r_1] \tag{2.20}$$

Note that this law feeds the measurement noise through the control back into the plant. This can significantly affect control performance. Since the control feeds back the vibration, this is a *closed–loop* control law, as opposed to the previous global formulation which is classified as an *open–loop* control law.

2.4 Global Cautious Control Law

The global cautious control law is obtained via the minimization of the stochastic performance function

$$J = E\,\{x^T x + u^T u(r_1) + \Delta u^T \Delta u(r_2) + u^T \Psi\Lambda + \Lambda^T \Psi^T u\} \tag{2.21}$$

where E { } is the expected value operator. By inserting in (2.2) and (2.3) this becomes

$$\begin{aligned} J = E\,\{&x_o^T x_o + u^T T^T x_o + u^T T^T T\,u + x_o^T\,T\,u\} \\ &+ u^T u(r_1 + r_2) + u_i^T u_i r_2 - u^T u_i r_2 - u_i^T u r_2 + u^T \Psi\Lambda + \Lambda^T \Psi^T u \end{aligned} \tag{2.22}$$

To obtain the solution, the expected value term must be expressed in terms of the available information state: $\bar{x}_{o_i}$, $\bar{T}_i$, $\bar{P}_i$. First, consider the *a priori* covariance matrix definition,

$$\bar{P}_i = E\{(\bar{\theta}_i - \theta_i)^T (\bar{\theta}_i - \theta_i)\} \tag{2.23}$$

$$\theta_i = \left[x_{o_i} \mid T_i \right]$$

The covariance matrix can be partitioned as

$$\bar{P}_i = \left[\begin{array}{c|c} \bar{P}_{11_i} & \bar{P}_{12_i} \\ \hline \bar{P}_{21_i} & \bar{P}_{22_i} \end{array} \right]$$

$$\bar{P}_{11_i} = E\{(\bar{x}_{o_i} - x_{o_i})^T (\bar{x}_{o_i} - x_{o_i})\} \equiv E\{\zeta_{x_i}^T \zeta_{x_i}\}$$

$$\bar{P}_{12_i} = E\{(\bar{x}_{o_i} - x_{o_i})^T (\bar{T}_i - T_i)\} \equiv E\{\zeta_{x_i}^T \zeta_{T_i}\}$$

$$\bar{P}_{21_i} = E\{(\bar{T}_i - T_i)^T (\bar{x}_{o_i} - x_{o_i})\} \equiv E\{\zeta_{T_i}^T \zeta_{x_i}\} \tag{2.24}$$

$$\bar{P}_{22_i} = E\{(\bar{T}_i - T_i)^T (\bar{T}_i - T_i)\} \equiv E\{\zeta_{T_i}^T \zeta_{T_i}\}$$

$$\zeta_{x_i} = \bar{x}_{o_i} - x_{o_i}$$

$$\zeta_{T_i} = \bar{T}_i - T_i \tag{2.25}$$

and the cycle i+1 and i plants are related by the filter's random walk model

$$\begin{aligned} \mathbf{x}_o &= \mathbf{x}_{o_i} + \mathbf{w}_{x_i} \\ \mathbf{T} &= \mathbf{T}_i + \mathbf{w}_{T_i} \end{aligned} \tag{2.26}$$

with $E\{\mathbf{w}_{x_i}^T \mathbf{w}_{x_i}\} = \mathbf{W}_{11}$, $E\{\mathbf{w}_{x_i}^T \mathbf{w}_{T_i}\} = \mathbf{0}_n^T$, $E\{\mathbf{w}_{T_i}^T \mathbf{w}_{x_i}\} = \mathbf{0}_n$, and $E\{\mathbf{w}_{T_i}^T \mathbf{w}_{T_i}\} = \mathbf{W}_{22}$ ($\mathbf{0}_n$ is a null n–vector. Note that the process noise here is stationary.). Using (2.25) and (2.26) the cycle i+1 quantities $\mathbf{x}_o$, $\mathbf{T}$ can be related to the cycle i information state,

$$\begin{aligned} \mathbf{x}_o &= \bar{\mathbf{x}}_{o_i} - \zeta_{x_i} + \mathbf{w}_{x_i} \\ \mathbf{T} &= \bar{\mathbf{T}}_i - \zeta_{T_i} + \mathbf{w}_{T_i} \end{aligned} \tag{2.27}$$

and the expected value term of (2.22) can be solved:

$$\begin{aligned} E\{\mathbf{x}_o^T \mathbf{x}_o\} = E\{&\bar{\mathbf{x}}_{o_i}^T \bar{\mathbf{x}}_{o_i} - \bar{\mathbf{x}}_{o_i}^T \zeta_{x_i} + \bar{\mathbf{x}}_{o_i}^T \mathbf{w}_{x_i} \\ &+ \zeta_{x_i}^T \zeta_{x_i} - \zeta_{x_i}^T \bar{\mathbf{x}}_{o_i} - \zeta_{x_i}^T \mathbf{w}_{x_i} \\ &+ \mathbf{w}_{x_i}^T \mathbf{w}_{x_i} - \mathbf{w}_{x_i}^T \zeta_{x_i} + \mathbf{w}_{x_i}^T \bar{\mathbf{x}}_{o_i}\} \end{aligned} \tag{2.28}$$

Since the estimate is a constant, it passes through the expected value operator. Therefore, with $\bar{\mathbf{x}}_{o_i}$ an unbiased estimate and $\mathbf{w}_x$ a zero mean random vector,

$$E\{\bar{\mathbf{x}}_{o_i}^T \zeta_{x_i}\} = \bar{\mathbf{x}}_{o_i}^T E\{\zeta_{x_i}\} = 0$$

$$E\{\bar{x}_{o_i}^T w_{x_i}\} = x_{o_i}^T E\{w_{x_i}\} = 0$$

and the random walk statistically independent of the estimate error,

$$E\{w_{x_i}^T \zeta_{x_i}\} = 0$$

(2.28) simplifies to

$$E\{x_o^T x_o\} = \bar{x}_o^T \bar{x}_{o_i} + E\{\zeta_{x_i}^T \zeta_{x_i}\} + E\{w_{x_i}^T w_{x_i}\}$$

$$E\{x_o^T x_o\} = \bar{x}_{o_i}^T \bar{x}_{o_i} + \bar{P}_{11_i} + W_{11} \tag{2.29}$$

Similarly,

$$\begin{aligned} E\{u^T T^T x_o\} &= u^T E\{T^T x_o\} \\ &= u^T E\{(\bar{T}_i - \zeta_{T_i} + w_{T_i})^T (\bar{x}_{o_i} - \zeta_{x_i} + w_{x_i})\} \\ &= u^T (\bar{T}_i^T \bar{x}_{o_i} - \bar{T}_i^T \zeta_{x_i} + \bar{T}_i^T w_{x_i} \\ &\quad + \zeta_{T_i}^T \zeta_{x_i} - \zeta_{T_i}^T \bar{x}_{o_i} - \zeta_{T_i}^T w_{x_i} \\ &\quad + w_{T_i}^T w_{x_i} - w_{T_i}^T \zeta_{x_i} + w_{T_i}^T \bar{x}_{o_i}\} \\ &= u^T (\bar{T}_i^T \bar{x}_{o_i} + E\{\zeta_{T_i}^T \zeta_{x_i}\} + E\{w_{T_i}^T w_{x_i}\}) \end{aligned}$$

$$E\{u^T T^T x_o\} = u^T (\bar{T}_i^T \bar{x}_{o_i} + \bar{P}_{21_i}) \tag{2.30}$$

and by the same methodology,

$$E\{u^T T^T T\, u\} = u^T(\bar{T}_i^T \bar{T}_i + \bar{P}_{22_i} + W_{22})\, u \tag{2.31}$$

Equations (2.29), (2.30), (2.31), and (2.30) transpose define all the terms in (2.22); therefore,

$$\begin{aligned} J = {} & (\bar{x}_{o_i}^T \bar{x}_{o_i} + \bar{P}_{11_i} + W_{11}) + u^T (\bar{T}_i^T \bar{x}_{o_i} + \bar{P}_{21_i}) \\ & + (\bar{x}_{o_i}^T \bar{T}_i + \bar{P}_{12_i})\, u + u^T (\bar{T}_i^T \bar{T}_i + \bar{P}_{22_i} + W_{22})\, u \\ & + u^T u(r_1 + r_2) + u_i^T u_i r_2 - u^T u_i r_2 - u_i^T u r_2 + u^T \Psi\Lambda + \Lambda^T \Psi u^T \end{aligned} \tag{2.32}$$

Taking the first variation yields

$$\begin{aligned} \partial J = {} & \partial u^T [(\bar{T}_i^T \bar{x}_{o_i} + \bar{P}_{21_i}) + (\bar{T}_i^T \bar{T}_i + \bar{P}_{22_i} + W_{22})\, u \\ & + u(r_1 + r_2) - u_i(r_2) + \Psi\Lambda] \\ & + \partial\Lambda^T [\Psi^T u] + [u^T \Psi]\, \partial\Lambda \\ & + [(\bar{x}_{o_i}^T \bar{T}_i + \bar{P}_{12_i}) + u^T (\bar{T}_i^T \bar{T}_i + \bar{P}_{22_i} + W_{22}) \\ & + u^T(r_1 + r_2) - u_i^T(r_2) + \Lambda^T \Psi^T]\, \partial u \end{aligned}$$

Setting this equal to zero results in the two equations:

$$\begin{aligned} & -[\bar{T}_i \bar{T}_i + \bar{P}_{22_i} + W_{22} + I(r_1 + r_2)]\, u = [\bar{T}_i^T \bar{x}_{o_i} + \bar{P}_{21_i} - u_i(r_2)] + \Psi\Lambda \\ & \Psi^T u = 0 \end{aligned} \tag{2.33}$$

These are the cautious analogues to the (2.6) equations and have the solution:

$$u_{i+1} = \{Z^{-1}\ \Psi\ [\Psi^T\ Z^{-1}\ \Psi]^{-1}\ \Psi^T - I\}\ Z^{-1}\ X$$

$$Z = [\overline{T}_i\ \overline{T}_i + I(r_1+r_2) + \overline{P}_{22_i} + W_{22}] \tag{2.34}$$

$$X = [\overline{T}_i^T\ \overline{x}_o - u_i(r_2) + \overline{P}_{21_i}] \tag{2.35}$$

This is the global cautious control law. Note the difference between these equations and (2.10) and (2.11). The addition of the covariance and process noise term in the Z matrix formulation acts like increased control quadratic weighting. This discourages large control vector magnitudes when the filter is uncertain about the impulse response matrix estimate. The cross covariance vector $\overline{P}_{21}$ in (2.35) acts the opposite of control rate quadratic weighting encouraging change most heavily in those elements of the control vector that are associated with large uncertainties in $T^T x_o$.

2.5 Local Cautious Control Law

By taking the first variation of the stochastic performance function of (2.21) with the local model substitutions (2.12) and setting it equal to zero, the following two equations are obtained:

$$-[E\ \{T^T T\} + I(r_1+r_2)]\ \Delta u = [E\ \{T^T x_i\} + u_i(r_1)] + \Psi\Lambda \tag{2.36}$$

As was found for the global cautious control law,

$$E\{T^T T\} = \bar{T}_i^T \bar{T}_i + \bar{P}_{22_i} + W_{22}$$

(where $\bar{P}_{22_i}$ is now the entire covariance matrix since the local model Kalman filter only estimates $\bar{T}_i$ and not $\bar{x}_{0_i}$) whereas the expected value term on the right side of (2.36) has not been encountered before. Immediately it comes to mind to replace x_i in this term with y_i since

$$E\{x_i\} = y_i$$

because the measurement noise is zero mean. However, the measurement vector y_i is not available to the end of the cycle i, while the control for cycle i+1 must be computed during cycle i. Therefore, the quantity x_i must be related to the previous measurement:

$$x_i = x_{i-1} + T_i \Delta u_i$$
$$x_i = y_{i-1} - v_{i-1} + T_i \Delta u_i$$

$$E\{T^T x_i\} = E\{T^T (y_{i-1} - v_{i-1} + T_i \Delta u_i\}$$

from (2.27)

$$T = \bar{T}_i - \zeta_{T_i} + w_{T_i}$$

$$E\{T^T x_i\} = E\{(\overline{T}_i^T - \zeta_{T_i}^T + w_{T_i}^T)(y_{i-1} - v_{i-1} + (\overline{T}_i - \zeta_{T_i})\,\Delta u_i)\}$$

Assuming the estimate errors are uncorrelated with the measurement noise

$$E\{T\,x_i\} = \overline{T}_i^T\,y_{i-1} + (\overline{T}_i^T\,\overline{T}_i + \overline{P}_{22_i})\,\Delta u_i$$

and the solution to (2.36) is

$$u_{i+1} = u_i + (Z^{-1}\,\Psi\,[\Psi^T\,Z^{-1}\,\Psi]^{-1}\,\Psi^T - I)\,Z^{-1}\,X$$

$$Z = [\overline{T}_i^T\,\overline{T}_i + I\,(r_1+r_2) + \overline{P}_{22_i} + W_{22}] \qquad (2.37)$$

$$X = [\overline{T}^T\,y_{i-1} + \overline{T}_i^T\,\overline{T}_i\,\Delta u_i + u_i(r_1) + \overline{P}_{22_i}\,\Delta u_i]$$

This control law contains covariance and process noise matrices not present in the local certainty equivalent control law in (2.20). The role of the covariance matrix in this equation is similar to that of the control quadratic weighting. Through the **Z** matrix equation, the uncertainty acts to decrease the change in the control, while through the **X** vector equation the uncertainty acts to excite changes in those modes of the control vector whose previous changes lied close to the larger principal axes of the covariance ellipsoid.

2.6 Performance of Certainty Equivalent and Cautious Controls

As pointed out by Bar–Shalom [50], cautious and certainty equivalent controls are best suited for different control problems. Cautious policies seek to

avoid the cost penalties associated with control of an unknown system. Thus, they function best on problems where the initial uncertainty is high and control is unlikely to result in better future estimates. Certainty equivalent controllers, while they do not actively probe the system like dual controllers, are more vigorous and thus incur both higher uncertainty costs and better estimates. If the system varies slowly enough and useful information can be extracted above the noise of signal, these controllers will improve their estimates and, therefore, their control. If the initial estimates are poor and the time horizon is sufficiently short, the exacerbation of the cost through the poor control will not be compensated by the later improvements in control due to better identification.

2.7 Inversion of the Z Matrix

One significant problem with the optimal control laws previously formulated is the inversion of the Z matrix. This matrix is mxm (where m is the size of the control vector, which is typically equal to n, the size of the measurement vector) and thus requires m^3 operations. For a quarter revolution cycle and vibrations harmonics up to 16Ω controlled, m must be at least an 8x1 vector by the Nyquist requirement. More realistically, the system should have at least four times this sampling frequency to yield proper control (m = 32). A matrix of this size could not be inverted in real time with present methods. This problem may be solved in several ways. With the advent of parallel computing and the increasing speed of processors, in the near future, matrices of this size may be invertible in real time.

Iterative routines exist, such as the Pan–Rief algorithm [60], which can quickly find a matrix inverse if supplied with a close approximation (such as the previous cycles Z^{-1}). The controller algorithm can be adjusted (for the cautious

case this would require re–derivation) so that the lag time between the obtaining of $\overline{T}_i$ and its use in the control is greater than the present one cycle. (The estimate $\overline{x}_{o_i}$ could still be used in computing the cycle i+1 control.) This method would lessen the vibration reduction obtained by the regulator in proportion to the quickness with which T changes.

Another method, which, while primitive, may work sufficiently well in the field would have the local Kalman filter identify T^{-1} (provided m=n). Then, if a certainty equivalent policy is used, the constraint condition is ignored, and no control or control–rate weight is used (which as shall be seen with the local model produces good control), then the control law becomes

$$u = u_i - (\overline{T^{-1}})_i \, y_{i-1}$$

where $(\overline{T^{-1}})_i$ is the *a priori* estimate of impulse response matrix inverse. This is a form of adaptive inverse control [61]. Note that no matrix inversion is required.

If the zero mean control constraint is dropped, the optimal control law (for both certainty equivalent and cautious policies) is

$$u = - Z^{-1} X$$

which is the solution of

$$Z u = -X$$

The optimal control u can be found in $n^3/3$ operations if it is not necessary to obtain Z^{-1}. Thus, a 66% reduction in the number of operations can be achieved. If the performance function is augmented with an orthogonality quadratic

$$u^T \Psi \Psi^T u(r_4)$$

and the weight r_4 is large, then the resulting control will approach the constrained control law. The **Z** matrix will then contain an orthogonality term:

$$Z = [\overline{T}_i^T \overline{T}_i + I (r_1 + r_2) + \Psi \Psi^T (r_4)]$$

As discussed in the previous chapter, the impulse response matrix is the product of a circulant matrix and a diagonal matrix. If the estimate could bc decomposed into these two parts, then the inversion of the nxn certainty equivalent **Z** matrix can be accomplished in O (n $\log_2$ n) operations if the control and control–rate weights are zero.

$$Z = [\overline{T}_i^T \overline{T}_i]$$

$$\overline{T}_i = \overline{C}_i \overline{B}_i \ , \qquad \overline{C}_i = \text{nxn circulant matrix}$$

$$\overline{B}_i = \text{nxn diagonal matrix}$$

$$Z = \overline{B}_i \overline{C}_i^T \overline{C}_i \overline{B}_i$$

Since $\overline{B}$ is diagonal it is invertible in n operations. Also, because the multiplication of two circulants yields a circulant and any circulant can be inverted in O (n $\log_2$ n) operations via FFT techniques, the computation of

$$Z^{-1} = \overline{B}_i^{-1} (\overline{C}_i^T \overline{C}_i)^{-1} \overline{B}_i^{-1}$$

can be completed in O (n $\log_2$ n). For n=32 this can result in 99% fewer operations than n^3 full matrix inversion. Note that the zero mean control constraint can still be used (as opposed to the previous method).

2.8 Output Constraint

A control constraint, $\mathbf{u}^T\Psi = 0$, was used in the previously defined performance functions to prevent control modes which would initiate rigid body motion. Since the azimuthal blade effectiveness is dependent on the flight condition, the elements of Ψ will vary during flight. Thus, any fixed control constraint, like that used in this paper, will be only approximately true at any time during flight. Another method to prevent control induced rigid body motion introduces an output constraint,

$$\mathbf{x}^T\Psi = 0$$

for the certainty equivalent performance function, or

$$E(\mathbf{x}^T\Psi) = 0$$

for the cautious performance function. After minimization, the control laws

$$\mathbf{u}_{i+1} = [Z^{-1}\bar{T}_i^T\Psi\,(\Psi^T\bar{T}_iZ^{-1}\bar{T}_i^T\Psi)^{-1}\,\Psi^T\,\bar{T}_i - I]\,Z^{-1}\,X \qquad \text{(global)}$$

$$\mathbf{u}_{i+1} = \mathbf{u}_i + [Z^{-1}\bar{T}_i^T\Psi\,(\Psi^T\bar{T}_iZ^{-1}\bar{T}_i^T\Psi)^{-1}\,\Psi^T\,\bar{T}_i - I]\,Z^{-1}\,X \qquad \text{(local)}$$

result. These are the equivalents of (2.7) and (2.18). The terms Z and X are the same as those derived in Sections 2.2, 2.3, 2.4, and 2.5 depending on the type of control law.

The prime disadvantage of the output constraint is that the efficacy of the

control (and the freedom from induced rigid body motion) is dependent on the accuracy of the impulse response matrix estimate. For this reason, it was rejected for this investigation.

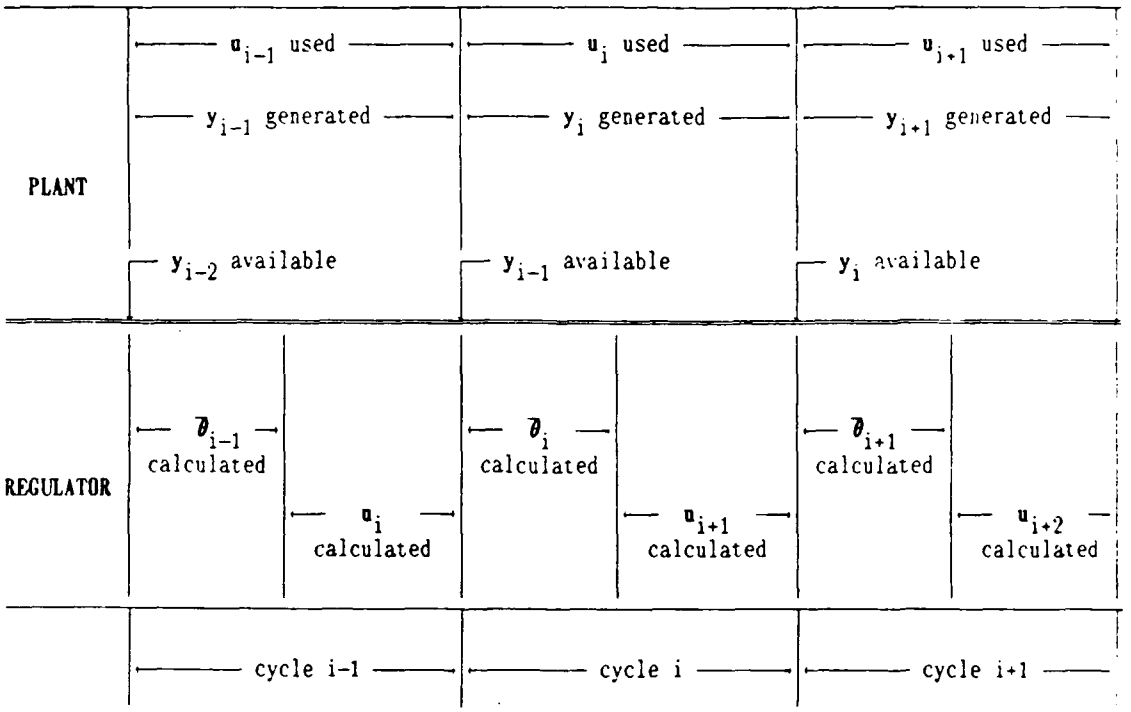

Figure 2.1 Time sequence for the plant, estimator, and controller

CHAPTER THREE: RESULTS, CONCLUSIONS, AND RECOMMENDATIONS

3.1 Introduction

The estimation and control algorithms developed in the previous two chapters were tested via simulation with the computer model described in Section 1.5. Several tests were designed to evaluate the performance of the filters and controllers. Open loop esitmation simulations were conducted first to establish an understanding of filter behavior. The closed loop regulators were then tested and analyzed. These results will be discussed but not presented here – for more detail please see Reference 63.

3.2 Simulation Results

The Kalman filter regulators consistently yielded between 89 and 93% vibration reduction in the simulations executed. Due to their superior noise suppression and better handling of uncontrolled vibration changes, the global Kalman filter regulators performed slightly better than their local counterparts.

The invariable global and local regulators produced fairly good results on most of the tests; in situations where there is little change in the plant, these can outperform the adaptive regulators. Since, for global Kalman filters, tunings that accentuate impulse response matrix tracking diminish uncontrolled vibration tracking and vice versa, it is highly desirable to base the tuning and filter model used on the types of plant changes most likely to be encountered. If the plant changes are concentrated in either one of $\mathbf{T}$ or $\mathbf{x}_0$, the optimal tuning regulator will in essence be invariable to the other. This fact may be used to reduce the computational burden of the filter and controller without degrading regulator

performance. For example, if the impulse response matrix changes very little under typical flight conditions, then a **T** invariable global regulator could be used providing quick response to changes in uncontrolled vibration with a simpler filter and an optimal control solution not requiring inversion of **Z**.

It is interesting to note that local regulators performed well when confronted with quick changes in uncontrolled vibration even though this change violates their formulations. This is at first confusing since open loop local estimators were weak in this area. But, the control variations produced by the changes in the plant resulted in increased identification prowess allowing for quick recovery. When the plant is changing slowly, the Kalman filter was found to track successfully. Thus, even with small control variations, useful information can be obtained about a noisy slowly drifting plant, permitting continuous vibration reduction. The closed loop regulator therefore appears to have avoided in practice its paradoxical kernel: for a stationary plant, full rank control is necessary for complete identification yet complete identification implies rank one control.

The batch weighted least squares filter regulators typically reduced vibrations 83 to 85% when optimally configured. The local WLS regulators performed better than its global counterpart due to the level of inaccuracy in the uncontrolled vibration estimate. For all but the random walk test, the optimal batch size was twelve. (In the random walk test the plant does not move as quickly away from its current state as in the other tests; therefore, a larger batch size improves identification.) This size exemplifies the classic principle of filter sensitivity: high sensitivity causes noise to be mistaken for information; low sensitivity causes information to be mistaken for noise. Neither in open loop or closed loop does the WLS filter identify as accurately as the Kalman filter. In the

open loop simulations this is largely due to measurement noise. The control constraint compounds this problem in the closed loop simulations.

Certainty equivalent control performance was degraded by the inclusion of any control weight. The use of a small control–rate weight resulted in greater vibration reduction for global regulators by limiting the control response to estimate errors (thus acting to filter out measurement noise). For local regulators, however, the control must remain free to follow changes in uncontrolled vibration not represented in the plant model quickly.

Cautious regulators even after retuning do not perform as well as certainty equivalent regulators. While they approach these levels of vibration reduction, they are still sluggish. Caution does yield some smoothing in behavior, but this can be achieved through control–rate weight and thereby the increased complexity of the cautious algorithms can be avoided.

Two methods were explored to prevent the control constraint induced covariance instability in the Kalman filter regulators. The first, random probing insertion, violates the control constraint deterministically but not statistically. This caps the covariance growth but degrades the vibration reduction performance. Philosophically, probing is poorly grounded since it cures a filter ailment through the corruption of the optimal control. The second method advanced, covariance trace bounding, alters the filter algorithm directly to prevent covariance instability. This method is justified by a simple truism: the difference between a filter estimate and the true value will always be well bounded. Covariance trace bounding was found to not degrade vibration reduction performance (unless, of course, the bound was unrealistically low). When this method was used with high process noise variance(s) the filter attained nearly fixed covariance eigenvalues. It may be

possible that the filter algorithm could use a fixed covariance matrix simplifying the computations of the Kalman gain vector and the estimate updates.

Any increase in measurement noise reduces identification accuracy and thereby vibration suppression. For the Kalman filter regulators, the degradation in vibration reduction is approximately linear in the measurement noise standard deviation over the range tested. When the noise had standard deviation 0.1 (ten times the baseline) the global Kalman filter regulator produced the best performance with 83% reduction while the local WLS filter regulator had the worst with only 68% vibration reduction. At this level of noise, the local filter regulators perform poorly since they feed the noise directly into the control.

The circulant estimation enhancement algorithm failed to improve the vibration reduction performances when added onto the filter algorithms even though it appeared to benefit estimation performance in the open loop simulations. This most likely resulted from losses in accuracy along some axes of the error ellipsoid while gains occurred along others. In some cases if the filter estimates were poor, the CEE algorithm would exacerbate the estimate errors. This resulted for a number of open loop and closed loop Kalman filter simulations in true instability. (Since the WLS algorithm is non–recursive, it is always stable.) This instability proved to be removable through re–tuning. The CEE global Kalman filter regulator did significantly outperform all other regulators in high noise testing. When a measurement noise standard deviation of 0.1 was used an additional 3% of vibration reduction was obtained. While the CEE algorithm presented in this report is clearly unacceptable due to its instability, many other ad hoc (possibly sub–optimal) algorithms could be formulated. One of these may yield better tracking as well as

noise suppression without either instability or undesirable complexity. An extended Kalman or full nonlinear filter could also be employed.

For greater detail on the open and closed loop results please see Reference 63.

3.3 Summary: The Impulse Response Method

A new method of tackling the helicopter vibration problem was demonstrated. The plant is characterized in terms of a discrete sequence of uncontrolled output and a matrix of impulse responses in order to fashion a discrete control sequence to minimize a performance function quadratic in the output. If the uncontrolled output is predictable and the plant dynamics, and therefore impulse response, are nearly stationary, then the output can be controlled with the assistance of an estimator. The periodicity of the helicopter plant yields the predictability of the uncontrolled output and sets the cycle length of the regulator. For the control of vertical vibration the cycle need only be one quarter of a blade revolution. If a nearly constant control condition is applied, the impulse responses in the matrix "wrap–around" producing a full matrix. This assumption, which is similar to the quasi–static assumption of higher harmonic control, produces a circulant matrix for systems with constant dynamics and a circulant–diagonal–product matrix for systems with periodic input coefficients. Circulant matrices can be diagonalized via Fast Fourier and inverse Fast Fourier transforms; therefore, the impulse response matrix formulation is directly related to both discrete time and frequency (HHC) domains. Both relationships, and the impulse response method itself, merit a theoretical investigation in their own right.

3.4 Summary: Kalman and Weighted Least Squares Filtering

Global and local Kalman filters were derived to estimate the plant parameters. The resulting algorithm was computationally simplified by the assumption of equivalent process and measurement noise covariances for each row of the plant variable matrix. Global and local batch weighted least squares (WLS) algorithms were also found. In regulator application the control constraint confounded the operation of the algorithms by preventing the matrix to be inverted from attaining full rank. This was solved by adding pseudo–random noise to the control vector so that the control constraint was kept in a statistical sense. A more elegant means to attain full rank might be to impose an additional constraint on the plant variable matrix.

It was demonstrated theoretically and experimentally that the stability of the Kalman filter covariance equation required a matrix of controls to have full rank. Furthermore, it was shown that the number of bounded covariance eigenvalues was equal to the rank. This simply means that if information is not received by the filter along an axis of the covariance ellipsoid then the uncertainty along this axis will grow due to the process noise covariance. This presented a problem to closed loop Kalman filter performance: the use of the control constraint guarantees that the control matrix will be less than full rank. Three solutions, covariance trace bounding, insertion of random noise, and filter turn–off/on, were offered. The first two of these were incorporated into the filter subroutines. (It is difficult to formulate a condition to allow the filter to turn–on again; also, this solution would disregard information along the axes that the control is actuating.)

The circulant/diagonal structure advanced for the impulse response matrix theoretically permits identification in two cycles. The filtering process, however,

must be considerably more complex since the model is nonlinear in these parameters. A regulator based upon this model would track changes in the plant with extreme agility although its stability would be questionable. The simplest identification algorithm for this nonlinear problem would be an extended Kalman filter.

In this research the circulant/diagonal structure of the impulse response matrix could be utilized without performing full nonlinear filtering by a method called circulant estimation enhancement (CEE). Here, the structure was imposed on the estimate supplied by the filter through an ad hoc algorithm. Many CEE algorithms could be derived including an optimal one which would require solving 2n nonlinear equations after each update.

3.5 Summary: Control Laws

Four optimal control laws employing the filter estimates were derived: the global certainty equivalent, the local certainty equivalent, the global cautious, and the local cautious. These were optimal with respect to an information state which was one cycle old. All the performance functions contained a zero mean control constraint to prevent vertical rigid body motion. The four control laws derived have an identical form because the constraint condition results in the removal of the undesired modes via a Householder transform. This constraint was an approximation since the actual lift generated by the four blades is a function of blade azimuth. However, this approximation allowed the constraint to be independent of the estimate accuracy and was therefore considered desirable. Considering the accuracy of the filter estimates maintained during the simulations presented, an output constraint dependent on the estimates may present no

problems to regulator performance whatsoever. In addition to restricting rigid body motion more accurately, the output constraint would not result in rank deficient control due to the random fluctuations in the estimates. Thus, a 'natural' probing would be present and the covariance equation of the Kalman filter would be stabilized. If WLS filtering was used, the control batch matrix would be of full rank despite the constraint.

The optimal control laws presented require the inversion of the mxm matrix **Z**. For multi–axis or high bandwidth vibration control this could not be performed in real time onboard as it requires O (n^3) operations. Several methods to overcome this problem were advanced including parallel computing algorithms, iterative routines, adaptive inverse control, and employment of the circulant/diagonal form. In the last of these methods, the inversion is possible in O ($n\log_2 n$) operations.

3.6 Recommendations

At this preliminary stage of research into the application of the impulse response method to the helicopter vibration problem, many different avenues of investigation are open and worthy of further study. Those of greatest import to the furtherance of the method are:

(1.) Continued Theoretical Development of the Impulse Response Method: The method, independent of application, needs to be firmly and completely connected to the body of control theory. Circulant relationships should be among the tools exploited in this process. Application to different types of systems (constant coefficients, periodic coefficient) should be examined.

(2.) Demonstration of the Method: The method should be tested in the control of a one degree of freedom dynamical system with a periodic forcing function and periodic coefficients. This should be compared to results of a higher harmonic control approach. An extended Kalman filter impulse response regulator using a circulant structure should also be tested.

(3.) Further Development of Helicopter Multi–Axes Models: These models should be developed in the complete context of blade dynamics and the rotor flow field so as to be understandable by the general helicopter community.

These recommendations are designed to remedy the skepticism and confusion of the helicopter community over this new control approach. Other areas of investigation such as the matrix inversion problem, output constraints in the performance function, and plant models that are not based on the nearly constant control assumption are certainly also of importance. But, advances in these areas will not appear to be of sufficient worth to pique the insular interests of the helicopter community. It is hoped that by expanding its theoretical base, demonstrating its application, and suggesting algorithms for actual helicopter implementation, the impulse response method will be received with increased interest.

REFERENCES

1. Loewy, R., "Helicopter Vibrations: a technological perspective," Journal of the American Helicopter Society, Vol. 29, No. 4, pp. 4–30, 1984.

2. McCloud, J. L., III, "The Promise of Multicyclic Control for Helicopter Vibration Reduction," Vertica, Vol. 4, No. 1, 1980.

3. Lewis, C. H., and Griffin, M. J., "A Review of the Effects of Vibration on Visual Acuity and Continuous Manual Control," Journal of Sound and Vibration, Vol. 56, No. 3, 1978.

4. International Standards Organization, Guide for the Evaluation of Human Exposure to Whole–Body Vibration, second edition, Ref. No. 150 2631–1978(E).

5. Griffin, M. J., Parsons, K. C., and Whitham, E. M., "Vibration and Comfort 4: Application of Experimental Results," Ergonomics, Vol. 25, No. 8, pp. 721–739, 1982.

6. Leatherwood, J. D., Clevenson, S. A., and Hollenbaugh, D. D., "Evaluation of Ride Quality Prediction Methods for Operational Military Helicopters," American Helicopter Society 39th Annual Forum, St. Louis, Mo., May 1983.

7. Landström, U., and Löfstedt, P., "Noise, Vibration and Changes in Wakefulness during Helicopter Flight," Aviation, Space, and Environmental Medicine, Feb. 1987.

8. Ham, N. D., and McKillip, R. M., "A Simple System for Helicopter Individual Blade Control and Its Application to Gust Alleviation," NASA Technical Paper 80–65, 1980.

9. Reichert, G., "Helicoter Vibration Control – A Survey," Vertica, Vol. 5, pp. 1–20, 1981.

10. McCloud, J. L., III, and Kretz, M., "Multicycle Jet–Flap Control for Alleviation of Helicopter Blade Stresses and Fuselage Vibration," Rotorcraft Dynamics, NASA SP–352, 1974, pp. 233–238.

11. Rand, O., "The Influence of Interactional Aerodynamics in Rotor/Fuselage Coupled Response," 2nd International Conference on Rotorcraft Basic Research, University of Maryland, Feb. 1988.

12. Friedmann, P. P., "Recent Developments in Rotary Wing Aeroelasticity," Journal of Aircraft, Vol. 14, No. 11, pp. 1027–1041, Nov. 1977.

13. Shaw, J. and Albion, N., "Active Control of the Helicopter Rotor for Vibration Reduction," 36th Annual Forum of the American Helicopter Society, Washington, D.C., May 1980.

14. Nguyen, K., and Chopra, I., "Actuator Power Requirements for Higher Harmonic Control (HHC) Systems," 2nd International Conference on Rotorcraft Basic Research, University of Maryland, Feb. 1988.

15. Wood, E. R. and Powers, R. W., "Practical Design Considerations for a Flightworthy Higher Harmonic Control System," Paper No. 80–57, American Helicopter Society 36th Annual Forum, Washington, D.C., May 1980.

16. Johnson, W., "Self Tuning Regulators for Multicyclic Control of Helicopter Vibration," NASA Technical Paper 1996, 1982.

17. Kretz, M., and Larche, M., "Future of Helicopter Rotor Control," Vertica, Vol. 4, pp. 13–322, 1980.

18. Wittenmark, B., "Stochastic Adaptive Control Methods: A Survey," International Journal of Control, Vol. 21, No. 5, 1975, pp. 705–730.

19. Chopra, I., and McCloud, J. L., III, "A Numerical Simulation Study of Open–Loop, Closed–Loop, and Adaptive Multicyclic Control Systems," Journal of the American Helicopter Society, Vol. 28, No. 1, January 1983.

20. Kretz, M., Aubrun, J. N., and Larche, M., "Wind Tunnel Tests of the Dorand DH 2011 Jet Flap Rotor," Vol. 1, NASA–CR–114693, 1973.

21. Kretz, M., Aubrun, J. N., and Larche, M., "Wind Tunnel Tests of the Dorand DH 2011 Jet Flap Rotor," Vol. 2, NASA–CR–114693, 1973.

22. McCloud, J. L., III, "An Analytical Study of a Multicyclic Controllable Twist Rotor," Paper No. 932, 31st Annual Forum of the American Helicopter Society, Washington, D.C., May 1975.

23. McCloud, J. L., III, and Weisbrich, A. L., "Wind Tunnel Test Results of a Full Scale Multicylic Controllable Twist Rotor," Paper No. 78–60, Annual Forum of the American Helicopter Society, Washington, D.C., May 1978.

24. Brown, T. J., and McCloud, J. L., III, "Multicyclic Control of a Helicopter Rotor Considering the Influence of Vibration, Loads, and Control Motion," Annual Forum of the American Helicopter Society, Washington, D.C., May 1980.

25. Sissingh, G. J., and Donham, R. E., "Hingeless Rotor Theory and Experiment on Vibration Reduction by Periodic Variation of Conventional Control," Rotorcraft Dynamics, NASA SP–352, pp. 2661–277, 1974.

26. Powers, R. W., "Application of Higher Harmonic Blade Feathering for Helicopter Vibration Reduction," NASA CR–158985, 1978.

27. Wood, E. R., Powers, R. W., and Hammond, C. E., "On Methods for the Applicaion of Harmonic Control," Vertica, Vol. 4, No. 1, 1980.

28. McHugh, F. J., and Shaw, J., Jr., "Benefits of Higher Harmonic Blade Pitch Vibration Reduction, Blade Load Reduction, and Performance Improvement," Proceedings of the American Helicopter Society Mideast Region Symposium on Rotor Technology, August 1976.

29. Shaw, J., and Albion, N., "Active Control of the Helicopter Rotor for Vibration Reduction," Paper No. 80–68, 36th Annual Forum of the American Helicopter Society, Washington, D.C., 1980.

30. Shaw, J., Jr., "Higher Harmonic Blade Pitch Control: A System for Helicopter Vibration Reduction," Ph.D. Thesis, Massachusetts Institute of Technology, May 1980.

31. Taylor, R. B., Farrar, F. A., and Miao, W., "An Active Control System for Helicopter Vibration Reduction by Higher Harmonic Pitch," Paper No. 80–71, 36th Annual Forum of the American Helicopter Society, Washington, D.C., May 13–15, 1980.

32. Taylor, R. B., Zwicke, P. E., Gold, P., and Miao, W., "Analytical Design and Evaluation of an Active Control System for Helicopter Vibration Reduction and Gust Response Alleviation," NASA CR–152377, 1980.

33. Hammond, C. E., "Wind Tunnel Results Showing Rotor Vibratory Loads Reduction Using Higher Harmonic Blade Pitch," 21st AIAA Structures, Structural Dynamics, and Materials Conference, Seattle, WA, 1980.

34. Molusis, J. A., Hammond, C. E., and Cline, J. H., "A Unified Approach to the Optimal Design of Adaptive and Gain Scheduled Controllers to Achieve minimum Helicopter Rotor Vibration," 37th Annual Forum of the American Helicopter Society, New Orleans, LA, May 1981.

35. Wood, E. R., Powers, R. W., Cline, J. H., and Hammond, C. E., "On Developing and Flight Testing a Higher Harmonic Control System," 39th Annual Forum of the American Helicopter Society, May 1983.

36. Wood, E. R., Powers, R. W., Cline, J. H., and Hammond, C. E., "On Developing and Flight Testing a Higher Harmonic Control System," Journal of the American Helicopter Society, Vol. 30, April 1985.

37. Molusis, J. A., "The Importance of Nonlinearity in the Higher Harmonic Control of Helicopter Vibration," 39th Annual Forum of the American Helicopter Society, St. Louis, MO, May 1983.

38. Davis, M. W, "Refinement and Evaluation of Helicopter Real–Time Self Adaptive Active Vibration Controller Algorithms," NASA Contractor Report No. 3821, 1984.

39. Jacklin, S. A., "Adaptive Inverse Control for Rotorcraft Vibration Reduction," NASA Technical Memorandum 83829, Oct. 1985.

40. Du Val, R. W., Gregory, C. Z., and Gupta, N. K., "Design and Evaluation of a State–Feedback Vibration Controller," Journal of the American Helicopter Society, Vol. 29, July 1984.

41. Gupta, N. K., "Frequency–Shaped Cost Functionals: Extension of Linear–Quadratic–Gaussian Design Methods," Journal of Guidance and Control, Vol. 3, No. 6, 1980, pp. 529–535.

42. Gupta, N. K., "Comparison of Frequency Domain and Time–Domain Rotorcraft Vibration Control Methds," NASA Contactor Report No. CR–166570, 1984.

43. Roy, R. H., Saberi, H. A., and Walker, R. A., "Fixed Gain and Adaptive Techniques for Rotorcraft Vibration Control," NASA CR–177344, May 1985.

44. Schrage, D. P., Oakes, G., and Jonnalagadda, V. R. P., "Development of an Individual Blade Control Computer Analysis," 2nd Technical Workshop on Dynamics and Aeroelastic Stability Modeling of Rotorcraft Systems, Boca Raton, FL, Nov. 1987.

45. Mendel, J. M., Lessons on Digital Estimation Theory, Prentice Hall, Inc., Englewood Cliffs, NJ, 1987.

46. Tapley, B. D., and Born, G. H., "Statistical Orbit Determination Theory," Center for Space Research, University of Texas, Austin, TX, Jan. 1985.

47. Sorenson, H. W., "An Overview of Filtering and Stochastic Control in Dynamic Systems," in Control and Dynamic Systems: Advances in Theory and Applications, C. T. Leondes, editor, Vol. 12, Academic Press, New York, pp. 1–61, 1976.

48. Bar–Shalom, Y. and Tse, E., "Concepts and Methods in Stochastic Control," in Control and Dynamic Systems: Advances in Theory and Applications, C. T. Leondes, editor, Vol. 12, Academic Press, New York, pp. 99–169, 1976.

49. Wieslander, J. and Wittenmark, B., "An Approach to Adaptive Control Using Real Time Identification," Automatica, Vol. 7, pp. 211–217, 1971.

50. Bar–Shalom, Y., Stochastic Dynamic Programming, Caution and Probing, IEEE Trans. on Automatic Control, AC–26, pp. 1184–1195.

51. D'Azzo, J. J. and Houpis, C. H., Linear Control System Analysis and Design, 2nd Edition, McGraw–Hill, New York, 1981.

52. Anderson, B. D. O. and Johnson, C. R., "Exponential Convergence of Adaptive Identification and Control Algorithms," Automatica, Vol. 18, No. 1, pp. 1–13, 1982.

53. Anderson, B. D. O., and Johnstone, R. M., "Adaptive Systems and Time Varying Plants," International Journal of Control, Vol. 37, pp. 367–377, 1983.

54. Anderson, B. D. O., "Adaptive Systems, Lack of Persistency of Excitation and Bursting Phenomena," Automatica, Vol. 21, No. 3, pp. 247–258, 1985.

55. Mendel, J. M., Discrete Techniques of Parameter Estimation: The Equation Error Formulation, Marce Dekker, New York, 1973.

56. Middleton, R. H. and Goodwin, G. C., "Adaptive Control of Time–Varying Linear Systems," IEEE Trans. on Automatic Control, Vol. 33, No. 2, Feb. 1988.

57. Jacklin, S. A., "Performance Comparison of Five Frequency Domain System Identification Techniques for Helicopter Higher Harmonic Control," 2nd International Conference on Rotorcraft Basic Research, University of Maryland, Feb. 1988.

58. Franklin, G. F., and Powell, J. D., Digital Control of Dynamic Systems, Addison–Wesley Publishing Co., Massachusetts, 1980.

59. Bryson, A. E., and Ho, Y. C., Applied Optimal Control: Optimization, Estimation, and Control, Hemisphere Publishing, New York, 1975.

60. Pan, V., and Reif, J., "Efficient Parallel Solution of Linear Systems," Proceedings of the 17th Annual ACM Symposium on Theory of Computing, Providence, RI, May 1985.

61. Jacklin, S. A., "Adaptive Inverse Control for Rotorcraft Vibration Reduction," NASA TM 86829, 1985.

62. Davis, P. J., Circulant Matrices, John Wiley & Sons, New York, 1979.

63. Knospe, C. R., "Adaptive Control of a System with Periodic Dynamics: Application of an Impulse Response Method to the Helicopter Vibration Problem," Ph.D. Dissertation, University of Virginia, May 1989.

DISTRIBUTION LIST

1 - 50	U. S. Army Research Office P. O. Box 12211 4300 S. Miami Boulevard Research Triangle Park, NC 27709 Attention: Richard O. Ulsh Chief, Information Processing Officer
51	Mr. Gary Anderson Technical Advisor U. S. Army Research Office P. O. Box 12211 4300 S. Miami Boulevard Research Triangle Park, NC 27709
*	Mr. Michael McCracken Administrative Contracting Officer Office of Naval Research Resident Representative 818 Connecticut Avenue Eighth Floor Washington, DC 20006
52 - 53	W. D. Pilkey, MAE
54	J. K. Haviland, MAE
55	M. A. Townsend, MAE
56 - 57	E. H. Pancake, Clark Hall
58	SEAS Preaward Administration Files

*Cover letter only

JO#2699:ph